Application of Geopolymers Modified with Chitosan as Novel Composites for Efficient Removal of Hg(II), Cd(II), and Pb(II) Ions from Aqueous Media

Ehab A. Abdelrahman[1] · Abdu Subaihi[2]

Abstract

In the present paper, two amorphous aluminum silicates (i.e. geopolymers) were synthesized via the interaction of 23.57 mmol of sodium metasilicate pentahydrate with 5.18 or 10.35 mmol of aluminum chloride hexahydrate. The synthesized geopolymers using 5.18 and 10.35 mmol of aluminum chloride hexahydrate were abbreviated as G1.25 and G2.50, respectively. Also, the synthesized geopolymers were modified with chitosan as novel composites. The synthesized composites using G1.25 and G2.50 were abbreviated as G1.25/Ch and G2.50/Ch, respectively. Besides, the synthesized geopolymers and their chitosan composites were characterized using different tools such as XRD, FT-IR, SEM, and EDX. Moreover, the synthesized geopolymers and their chitosan composites were utilized as efficient adsorbents for the removal of Hg(II), Cd(II), and Pb(II) ions from aqueous media. The Langmuir isotherm and pseudo-first-order kinetic model were more consistent with the removal of metal ions from aqueous media. Furthermore, the adsorption processes were spontaneous, exothermic, and chemisorption. In the case of Hg(II), the maximum adsorption capacity of G1.25, G2.50, G1.25/Ch, and G2.50/Ch were 131.93, 140.85, 166.67, and 173.91 mg/g, respectively. In the case of Cd(II), the maximum adsorption capacity of G1.25, G2.50, G1.25/Ch, and G2.50/Ch were 118.34, 134.95, 159.49, and 166.11 mg/g, respectively. In the case of Pb(II), the maximum adsorption capacity of G1.25, G2.50, G1.25/Ch, and G2.50/Ch were 102.15, 118.91, 128.21, and 156.01 mg/g, respectively.

Keywords Metal ions · Adsorption · Geopolymers · Composites

1 Introduction

Water is the foundation of life on earth. Water makes up about 60% of the human body's weight. Also, water is essential for all cells, organs, and tissues of the body. Besides, water is a fundamental asset for producing clothing and food [1]. So, safe drinking water is significant everywhere throughout the world. The industrial releasing of tremendous amounts of hurtful chemicals into water escalates the water crisis [2]. Pollutants can be classified into four classes: biological, chemical, physical, and radiological [3–7]. Physical toxins principally impact the physical properties of water such as appearance, sedimentation, and suspension of materials in the water. Biological contaminations are microorganisms or microbiological poisons such as parasites, viruses, and bacteria. Radiological toxins are elements with unsteady atoms that can emit ionizing radiation such as uranium, plutonium, and cesium. Chemical toxins are compounds which can be normally happening or man-made such as bleaching products, drugs, metals, pesticides, beauty care products, and phytosanitary products. Heavy metals are elements with a specific gravity more than 5.0, and atomic weights in the range 63.5–200.6 [8, 9]. These days, the overwhelming metal contamination of water is the most significant problems undermining human life because of the portability of these poisons in the water resources. With the fast advancement of industries, for example, batteries, mining, tanneries, metal plating, pesticides, and paper, heavy metal ions are straightforwardly or indirectly released into lakes, rivers, or sea environments [10–12]. The heavy metal ions are steady ecological contaminants since they can't be

✉ Ehab A. Abdelrahman
    dr.ehabsaleh@yahoo.com; ehab.abdelrahman@fsc.bu.edu.eg

1   Chemistry Department, Faculty of Science, Benha University, Benha 13518, Egypt

2   Department of Chemistry, Al-Qunfudhah University College, Al-Qunfudhah, Kingdom of Saudi Arabia

corrupted and devastated. Poisonous heavy metals ions, for example, As(III), Cu(II), Zn(II), Ni(II), Cd(II), Cr(III), Hg(II), and Pb(II) can be hurtful to water and furthermore remain a genuine general health problem. As(III) ions can cause skin and lung cancers. Also, Hg(II) ions can cause weakness of aspiratory and kidney function, dyspnea, and chest pain. Pb(II) ions can cause extreme dysfunction in the liver, kidneys, and reproductive system. Cd(II) ions can cause osteoporosis, kidney damage, high blood pressure, and destruction of testicular tissue or red blood cells [1, 13–17]. Numerous strategies, for example, physical precipitation, chemical precipitation, electrochemical, membrane filtration, solvent extraction, reverse osmosis, and adsorption are widely utilized for expelling heavy metal ions from aqueous media [1, 18–21]. Among

different procedures for expelling heavy metal ions from aqueous media, adsorption is viewed as one of the most conceivable and powerful systems for water treatment. Adsorption has been observed to be better than different techniques in terms of adaptability and effortlessness of configuration, starting cost, simplicity, and harshness toward lethal poisons. Besides, it doesn't bring unsafe substances [1, 22–25]. Different inorganic adsorbents such as titanium dioxide, silicon dioxide, manganese oxide, zinc oxide, hematite, carbon nanotubes, graphene oxide, magnetic graphene, hydroxyapatite, geopolymers, and zeolites are the most generally utilized for the expulsion of heavy metal ions from aqueous media [1, 26–39]. In late decades, polymeric adsorbents have risen as potential options in contrast to conventional adsorbents in terms of
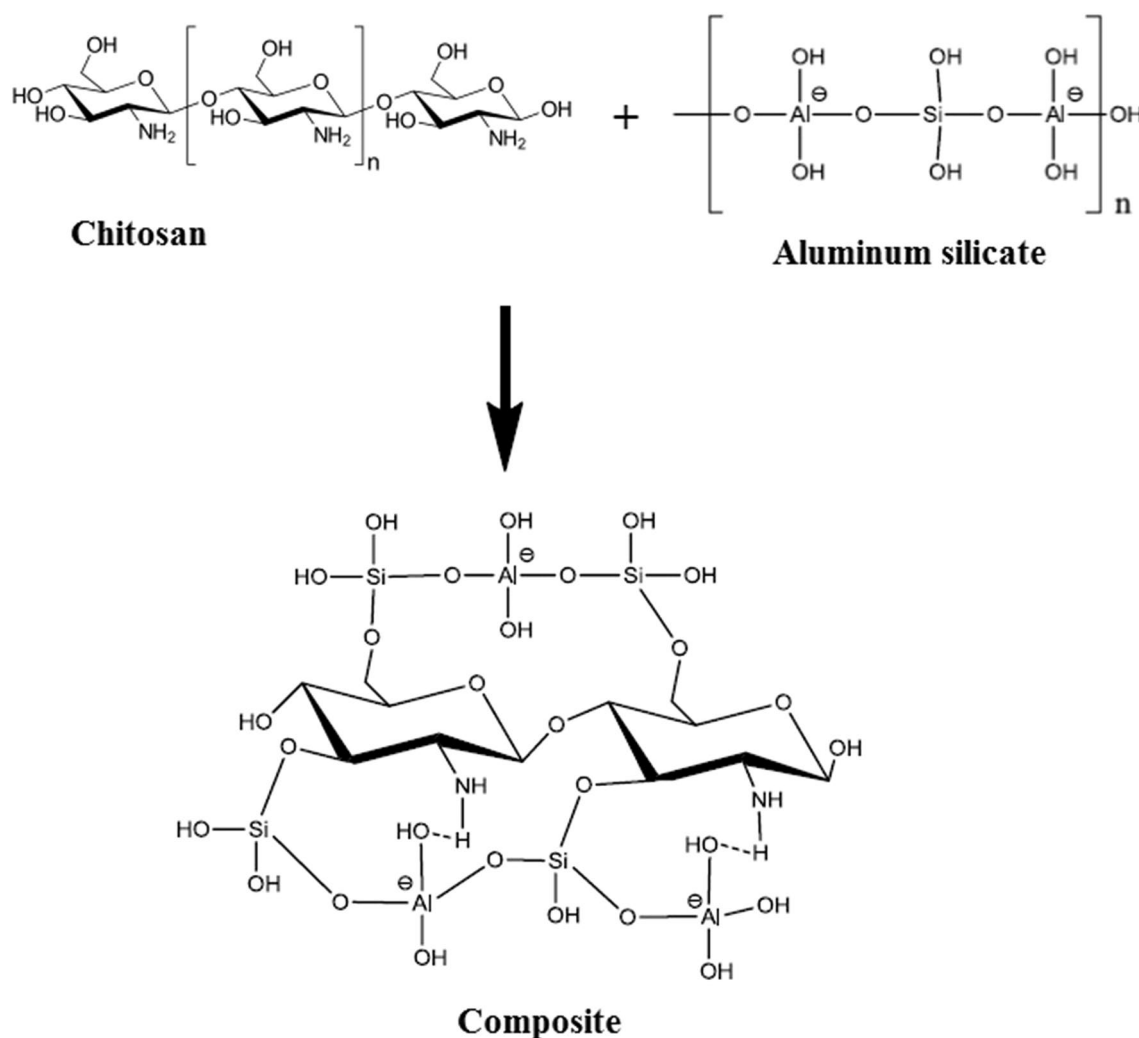

Scheme 1 Proposed structure of the chitosan/aluminum silicate composites according to Tiburu et al.

their immense surface area, pore size distribution, flexible surface, mechanical rigidity, and achievable recovery under gentle conditions. Carbohydrate polymers such as dextran, starch, cellulose, chitosan, and alginate are made out of long chains of monosaccharide units bound together by glycosidic linkages [1, 22, 23]. Also, carbohydrate polymers possess amine, hydroxyl, carboxyl, and amide functional groups which can capture the heavy metal ions. Composite materials, which composed of organic polymer and inorganic substance, are another gathering of adsorbents which were utilized essentially for the exclusion of heavy metal ions from aqueous media. Composite materials such as chitosan/zeolite, polypyrrole/Fe_3O_4, polypyrrole/TiO_2, and polythiophene/Sb_2O_3 show better adsorption capacities, chemical stabilities, and reproducibilities compared to pure inorganic and organic materials [1, 22, 23]. The gelation method was utilized for the production of geopolymers via three steps. The first step is the dissolving of aluminum and silicon precursors. The second step is the condensation for generating a –Si–O–Al–O– monomer. The third step is gel production through polycondensation for generating repeating units of –Si–O–Al–O– [40, 41]. Tiburu et al. showed the proposed structure of chitosan-aluminum silicate composites as clarified in Scheme 1 [42]. In this paper, geopolymer/chitosan composites were synthesized and utilized for the removal of Hg(II), Pb(II), and Cd(II) ions from aqueous media.

2 Experimental

2.1 Materials

Aluminum chloride hexahydrate ($AlCl_3 \cdot 6H_2O$), sodium metasilicate pentahydrate ($Na_2SiO_3 \cdot 5H_2O$), mercury(II) chloride ($HgCl_2$), cadmium(II) chloride ($CdCl_2$), ethylenediaminetetraacetic acid tetrasodium salt dihydrate ($C_{10}H_{16}N_2Na_4O_{10}$), glacial acetic acid ($CH_3COOH$), and lead(II) chloride ($PbCl_2$) were obtained from Sigma Aldrich company. Also, hydrochloric acid (HCl) was obtained from EL-Nasr Egyptian Company. Besides, sodium hydroxide (NaOH) was obtained from El-Gomhoria Egyptian Company. In addition, chitosan was obtained from ROTH Germany Company.
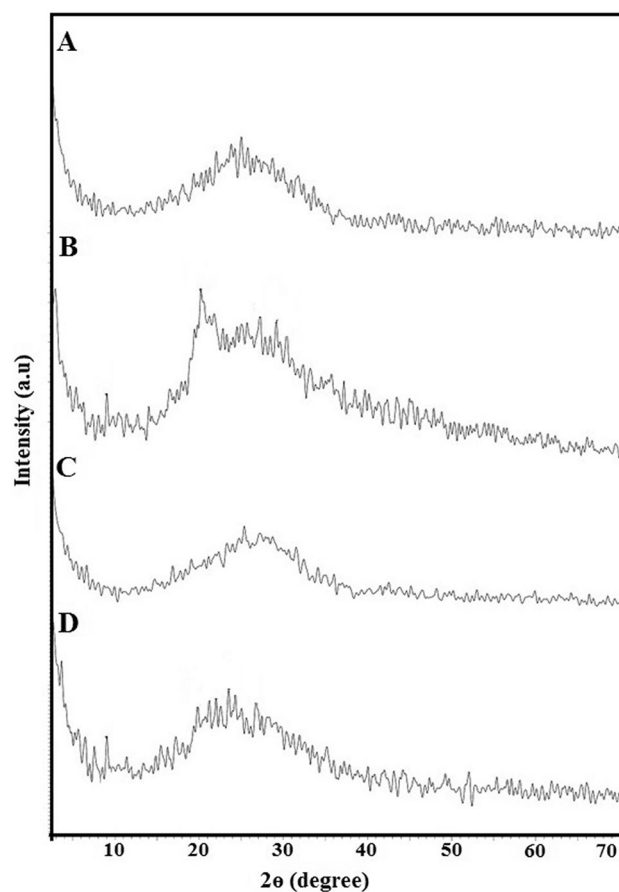
Fig. 1 XRD of G1.25 (A), G1.25/Ch (B), G2.50 (C), and G2.50/Ch (D) samples

2.2 Synthesis of Geopolymers

The aluminum solution was prepared as the following: 1.25 g (5.18 mmol) or 2.50 g (10.35 mmol) of aluminum chloride hexahydrate was dissolved in 35 mL of distilled water. Also, the silicon solution was prepared as the following: 5.00 g (23.57 mmol) of sodium metasilicate pentahydrate was dissolved in 35 mL distilled water. Then, the aluminum solution was added to the silicon solution drop by drop with constant stirring for 30 min. After that, the formed precipitate was filtered, washed several times with hot distilled water, and dried at 60 °C for 2 days. The products which were synthesized using 1.25 and 2.50 g of aluminum chloride hexahydrate were named G1.25 and G2.50, respectively.
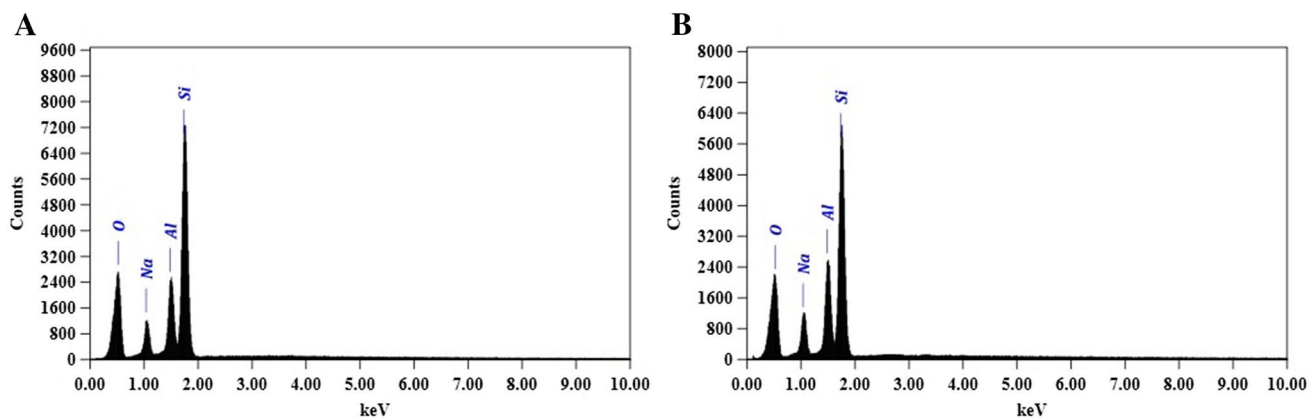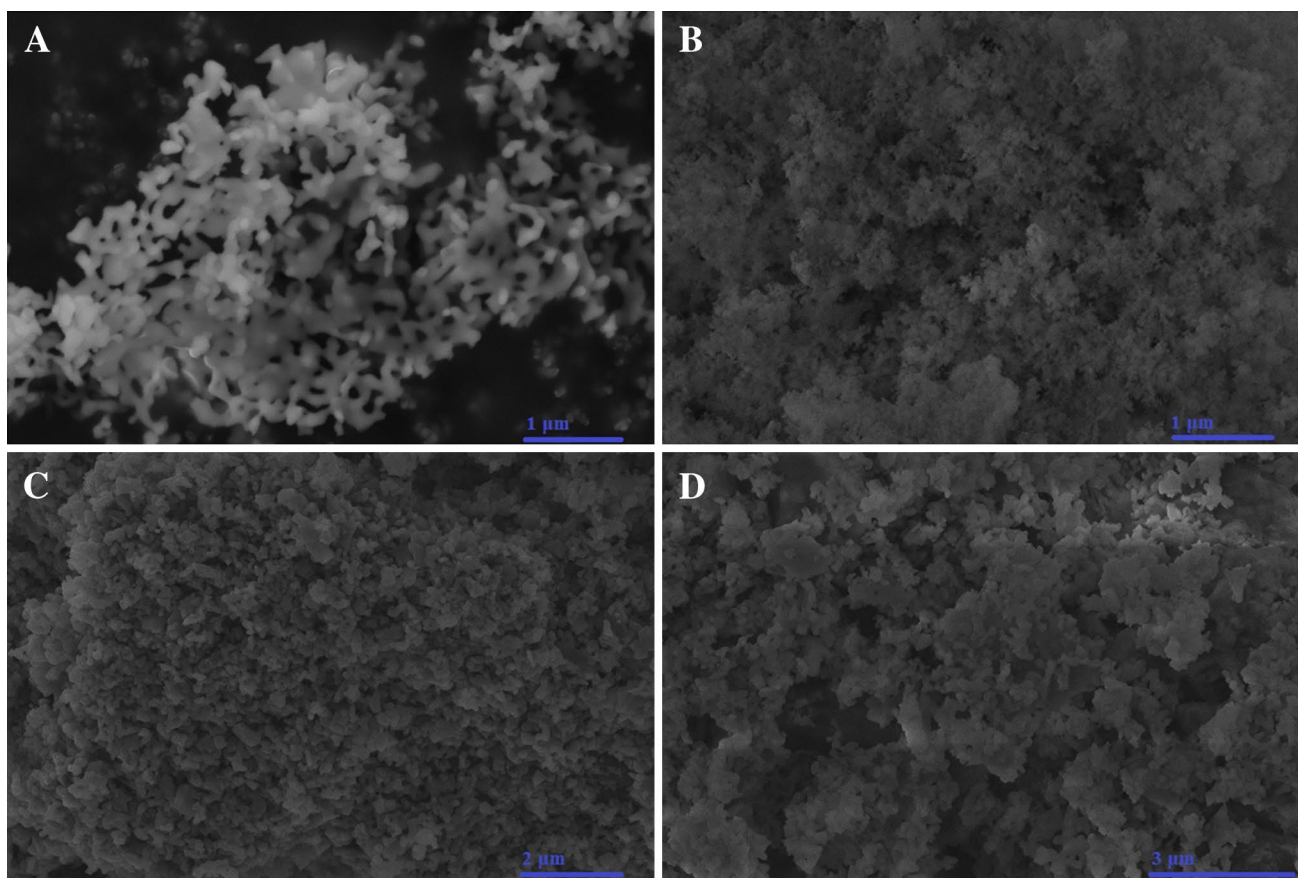
Fig. 2 EDS of G1.25 (**a**) and G2.50 (**b**) samples

Fig. 3 FE-SEM images of G1.25 (**a**), G2.50 (**b**), G1.25/Ch (**c**), and G2.50/Ch (**d**) samples

2.3 Synthesis of Geopolymer/Chitosan Composites

2 g of G1.25 or G2.50 and chitosan were added to 125 mL of 1.04 M acetic acid solution then were stirred at 900 rpm for 6 h. After that, the resulting mixture was added partially wise to 250 mL of 0.65 M sodium hydroxide solution then were stirred at 900 rpm for 6 h. In addition, the formed composite was filtered, washed several times with
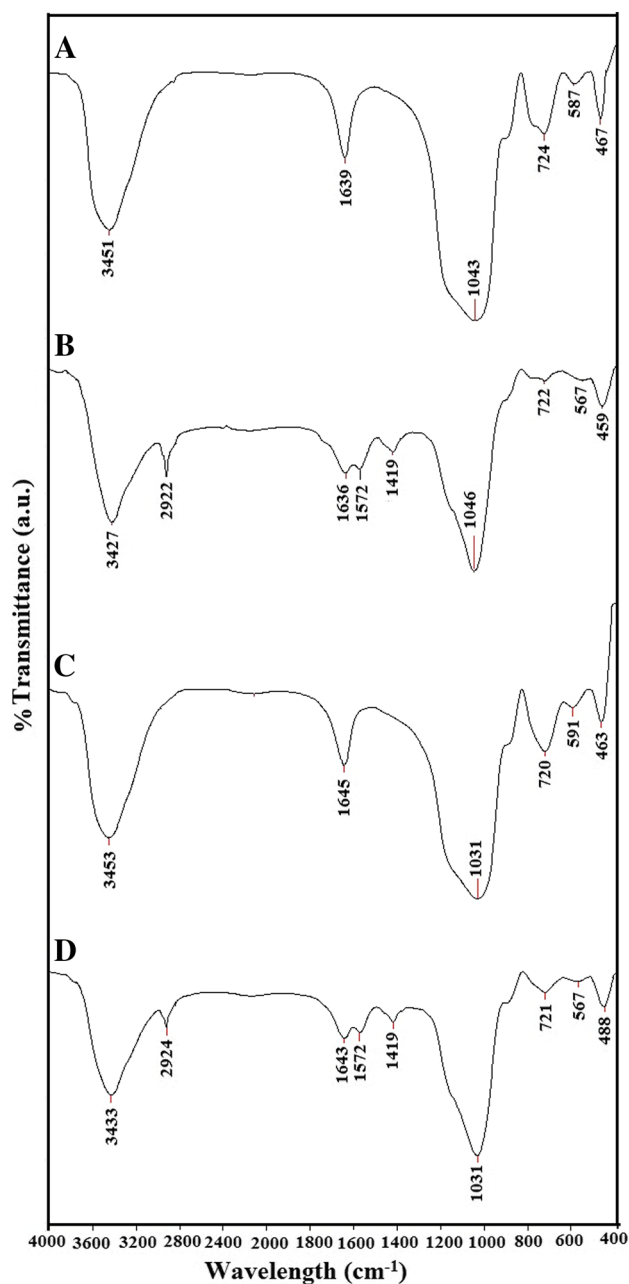
Fig. 4 FT-IR of G1.25 (A), G1.25/Ch (B), G2.50 (C), and G2.50/Ch (D) samples

hot distilled water, dried at 60 °C for 2 days, and grinded using agate mortar. The composites which were synthesized using G1.25 and G2.50 were named G1.25/Ch and G2.50/Ch, respectively.

2.4 Removal of Hg(II), Pb(II), and Cd(II) Ions from Aqueous Media Using the Synthesized Products

Adsorption experiments using G1.25, G2.50, G1.25/Ch, and G2.50/Ch adsorbents were performed for evaluating the removal of Hg(II), Pb(II), and Cd(II) ions from aqueous media. The effect of pH experiments was performed by shaking 0.12 g of G1.25, G2.50, G1.25/Ch, or G2.50/Ch with 60 mL of 500 mg/L pH-controlled Hg(II), Pb(II), or Cd(II) solution for 3 h. After that, the adsorbent was filtered then the concentration of Hg(II), Pb(II), or Cd(II) ions in the filtrate was estimated utilizing atomic absorption spectrometer. The pH of the working solutions was controlled using diluted solutions of sodium hydroxide and hydrochloric acid. The effect of time experiments was performed by shaking 0.12 g of G1.25, G2.50, G1.25/Ch, or G2.50/Ch with 60 mL of 500 mg/L Hg(II), Pb(II), or Cd(II) solution at pH 8 for a specific time at room temperature (298 K). After that, the adsorbent was filtered then the concentration of Hg(II), Pb(II), or Cd(II) ions in the filtrate was estimated utilizing atomic absorption spectrometer. The effect of temperature experiments was performed by shaking 0.12 g of G1.25, G2.50, G1.25/Ch, or G2.50/Ch with 60 mL of 500 mg/L Hg(II), Pb(II), or Cd(II) solution at pH 8 for 60 min at different temperatures (298–328 K). After that, the adsorbent was filtered then the concentration of Hg(II), Pb(II), or Cd(II) ions in the filtrate was estimated utilizing atomic absorption spectrometer. The effect of concentration experiments was performed by shaking 0.12 g of G1.25, G2.50, G1.25/Ch, or G2.50/Ch with 60 mL of different concentrations of Hg(II), Pb(II), or Cd(II) ions at pH equals 8 for 60 min at room temperature (298 K). After that, the adsorbent was filtered then the concentration of Hg(II), Pb(II), or Cd(II) ions in the filtrate was estimated utilizing atomic absorption spectrometer.

The % removal of Hg(II), Pb(II), or Cd(II) ions using G1.25, G2.50, G1.25/Ch, or G2.50/Ch was determined according to Eq. (1).

$$\% \text{ removal} = (C_0 - C_e) \times 100 / C_0 \tag{1}$$

The amount of Hg(II), Pb(II), or Cd(II) ions adsorbed by G1.25, G2.50, G1.25/Ch, or G2.50/Ch was determined according to Eq. (2).

$$Q = (C_0 - C_e) V/m \tag{2}$$

where, Q (mg/g) is the capacity of G1.25, G2.50, G1.25/Ch, or G2.50/Ch, V(L) is the volume of the Hg(II), Pb(II), or Cd(II) solution, C_o (mg/L) is the initial concentration of

A

B

C
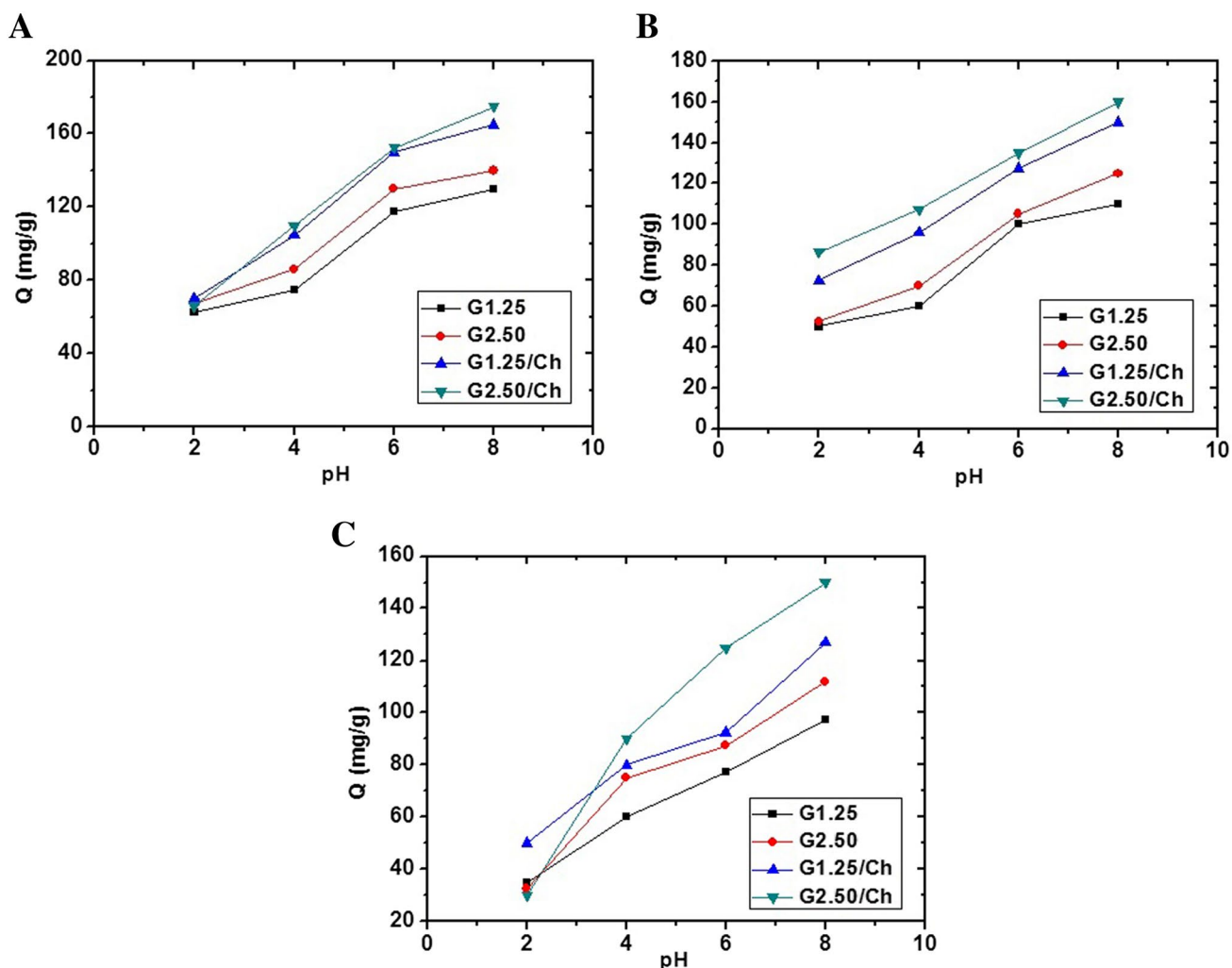
Fig. 5 Relation between adsorption capacity and pH for the removal of Hg(II) (**a**), Cd(II) (**b**), and Pb(II) (**c**) ions from aqueous media

Hg(II), Pb(II), or Cd(II) ions, C_e (mg/L) is the equilibrium concentrations of Hg(II), Pb(II), or Cd(II) ions, and m (g) is the dry weight of G1.25, G2.50, G1.25/Ch, or G2.50/Ch. In desorption process, Hg(II), Pb(II), or Cd(II) ions-loaded G1.25, G2.50, G1.25/Ch, or G2.50/Ch were mixed with 50 ml of 0.2 M ethylenediaminetetraacetic acid tetrasodium salt dihydrate then shaked for 6 h. Then, the adsorbents were filtered, washed with distilled water, and dried at 60 °C for 24 h. After that, the regenerated G1.25, G2.50, G1.25/Ch, or G2.50/Ch were reused three times to test the capacity for Hg(II), Pb(II), or Cd(II) ions under the same adsorption condition.

2.5 Characterization

XRD of G1.25, G2.50, G1.25/Ch, and G2.50/Ch samples was performed using X-ray diffractometer (Bruker, D8 Advance, and wavelength of Cu K_α irradiation equals 0.15 nm). Perkin Elmer FT-IR spectrophotometer was utilized for obtaining the spectra of G1.25, G2.50, G1.25/Ch, and G2.50/Ch samples in the range 4000–400 cm^{-1}. FE-SEM images of the G1.25, G2.50, G1.25/Ch, and G2.50/Ch samples were obtained using FEI QUANTA FEG 250 ultra-high resolution microscope equipped with an energy-dispersive X-ray spectrometer.
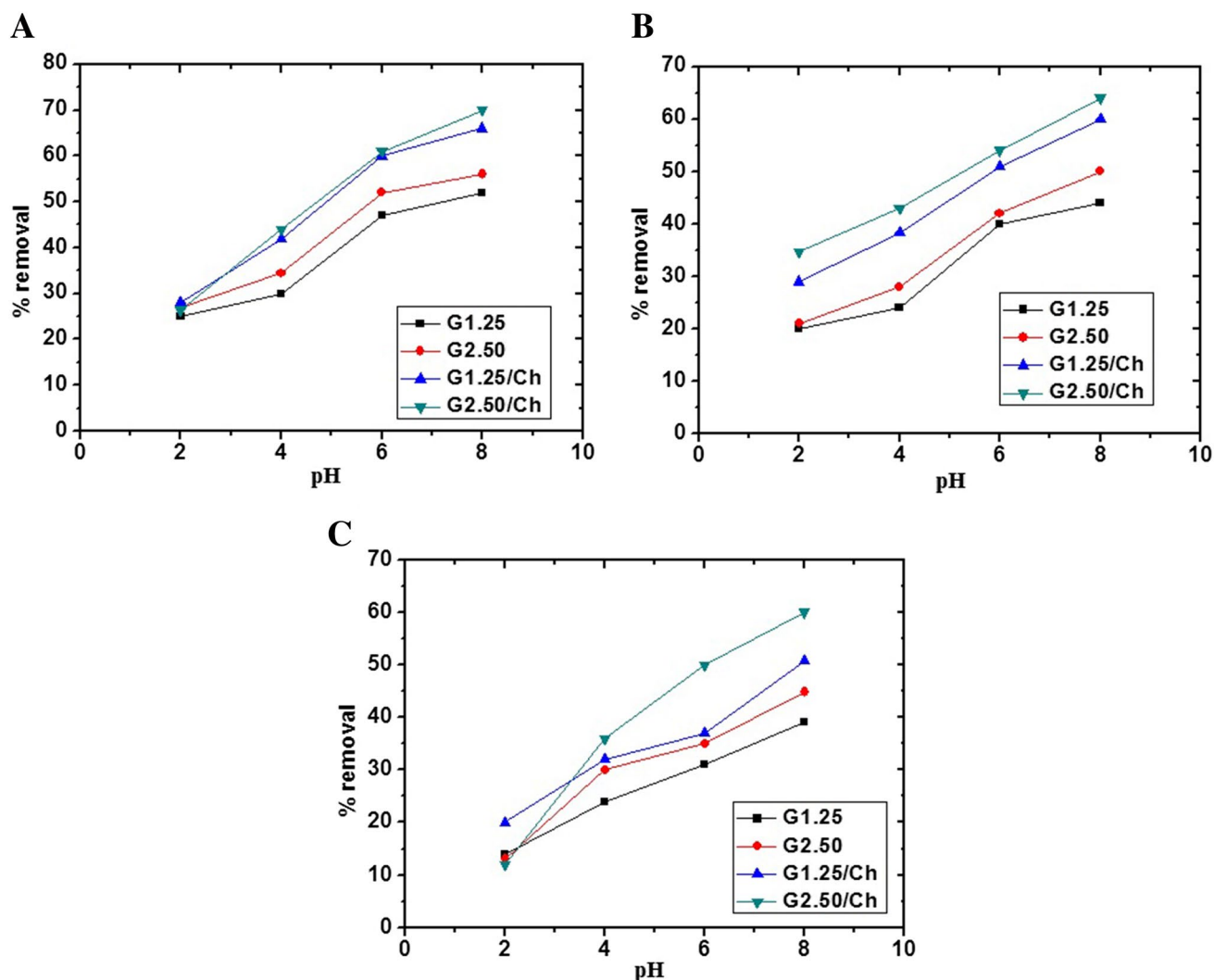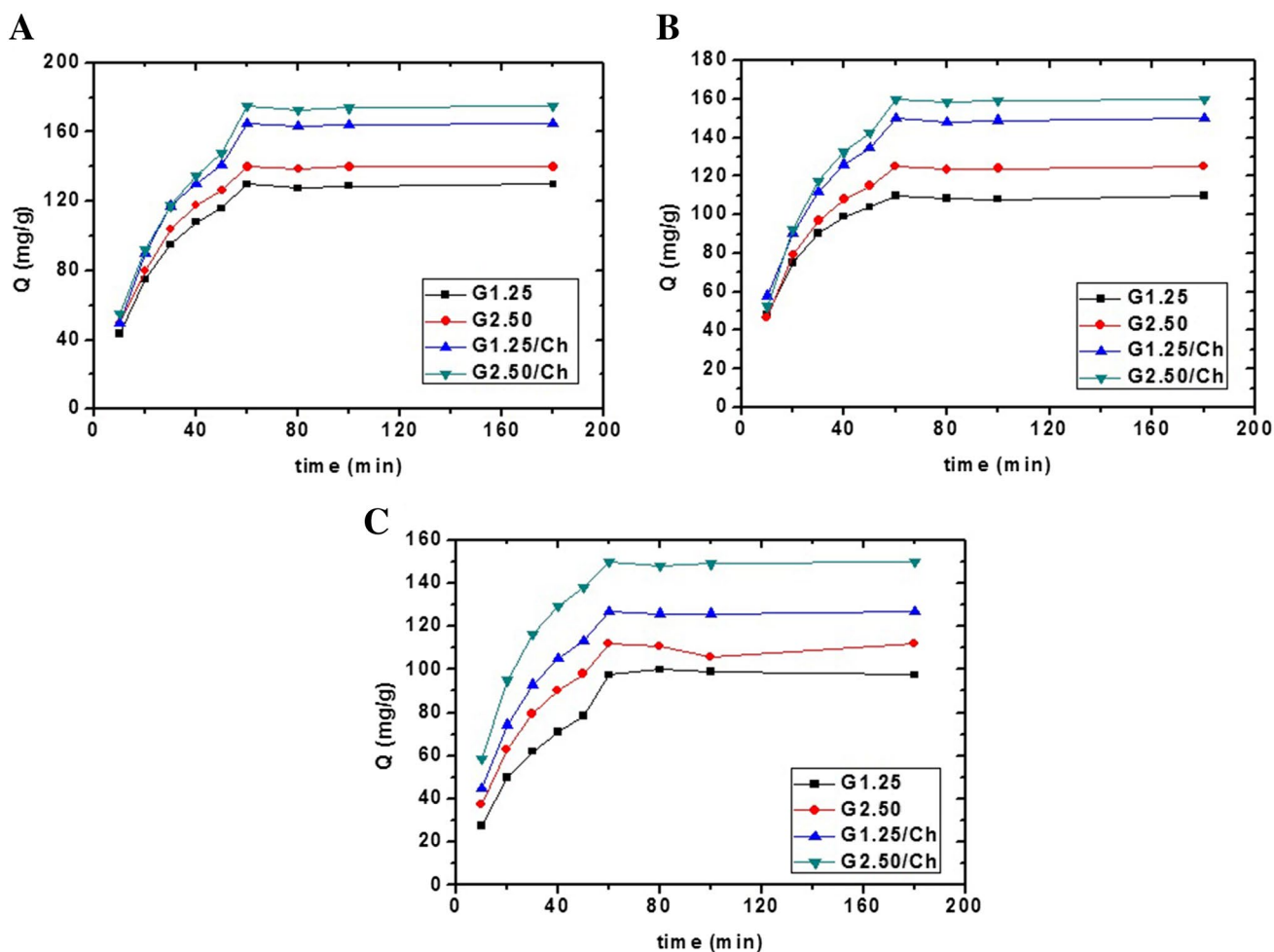
Fig. 6 Relation between pH and % removal of Hg(II) (**a**), Cd(II) (**b**), and Pb(II) (**c**) ions from aqueous media

3 Results and Discussion

3.1 Characterization of the Synthesized Products

X-ray diffraction analysis demonstrated the non-crystalline nature of the geopolymer samples (G1.25 and G2.50) and their chitosan composites (G1.25/Ch and G2.50/Ch). Broadband appeared in G1.25, G1.25/Ch, G2.50, and G2.50/Ch samples in the range $2\theta = 20°–30°$ as shown in Fig. 1a–d, respectively [22, 23, 40]. Energy-dispersive X-ray spectroscopy elucidated that the G1.25 sample composed of Si (39.45%), Al (12.42%),

Na (9.05), and O (39.08%) as shown in Fig. 2a. Also, G2.50 sample composed of Si (38.22%), Al (14.13%), Na (9.96), and O (37.69%) as shown in Fig. 2b. FE-SEM demonstrated that the G1.25 sample composed of sphere and irregular shapes as shown in Fig. 3a. Also, the G2.50 sample composed of cotton-like shapes as shown in Fig. 3b. Besides, G1.25/Ch and G2.25/Ch samples composed of flaky and irregular shapes as shown in Fig. 3c–d, respectively. Figure 4a–d represents FT-IR spectra of G1.25, G1.25/Ch, G2.50, and G2.25/Ch samples, respectively. The peaks which were observed at 467 and 463 cm^{-1} in the G1.25 and G2.25 samples are due to T–O–T bending

Fig. 7 Relation between adsorption capacity and time for the removal of Hg(II) (**a**), Cd(II) (**b**), and Pb(II) (**c**) ions from aqueous media

vibrations (T = Si and/or Al), respectively. Also, the peaks which were observed at 587 and 591 cm^{-1} in the G1.25 and G2.25 samples are due to internal T–O–T symmetric vibrations, respectively. Besides, the peaks which were observed at 724 and 720 cm^{-1} in the G1.25 and G2.25 samples are due to external T–O–T symmetric vibrations, respectively. Moreover, the peaks which were observed at 1043 and 1031 cm^{-1} in the G1.25 and G2.25 samples are due to external T–O–T asymmetric vibrations, respectively. The peaks which were observed at 1639 cm^{-1} and 1645 cm^{-1} in the G1.25 and G2.25 samples are due to bending vibrations of adsorbed water, respectively. Furthermore, the peaks which were observed at 3451 and 3453 cm^{-1} in the G1.25 and G2.25 samples are due to stretching vibrations of adsorbed water, respectively. The peaks which were observed at 459, 567, 722, and 1046 cm^{-1}

(in the case of G1.25/Ch) or at 448, 567, 721, and 1031 cm^{-1} (in the case of G2.50/Ch) are due to geopolymers. The peaks which were observed at 1419 cm^{-1} in the G1.25/Ch or G2.50/Ch samples are due to C–O bending vibrations. The peaks which were observed at 1572 cm^{-1} in the G1.25/Ch or G2.50/Ch samples are due to NH$_3^+$ deformation. The peaks which were observed at 1636 and 1643 cm^{-1} in the G1.25/Ch and G2.50/Ch samples are due to bending vibrations of adsorbed water and/or amino groups. The peaks which were observed at 3427 and 3433 cm^{-1} in the G1.25/Ch and G2.50/Ch samples are due to stretching vibrations of OH and/or NH groups. The peaks which were observed at 2922 and 2924 cm^{-1} in the G1.25/Ch and G2.50/Ch samples are due to stretching vibrations of C–H [22, 23, 40, 43].
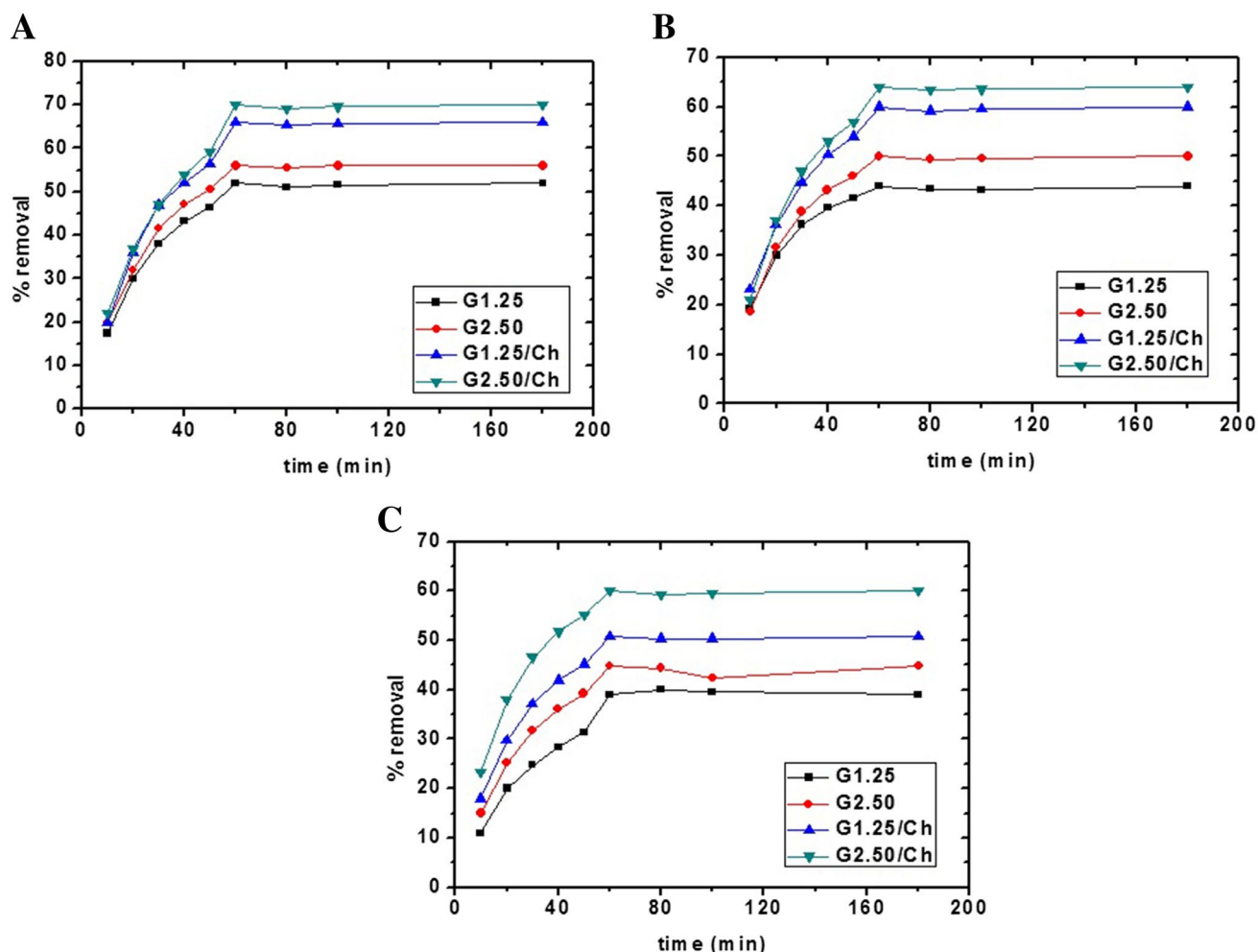
Fig. 8 Relation between time and % removal of Hg(II) (**a**), Cd(II) (**b**), and Pb(II) (**c**) ions from aqueous media
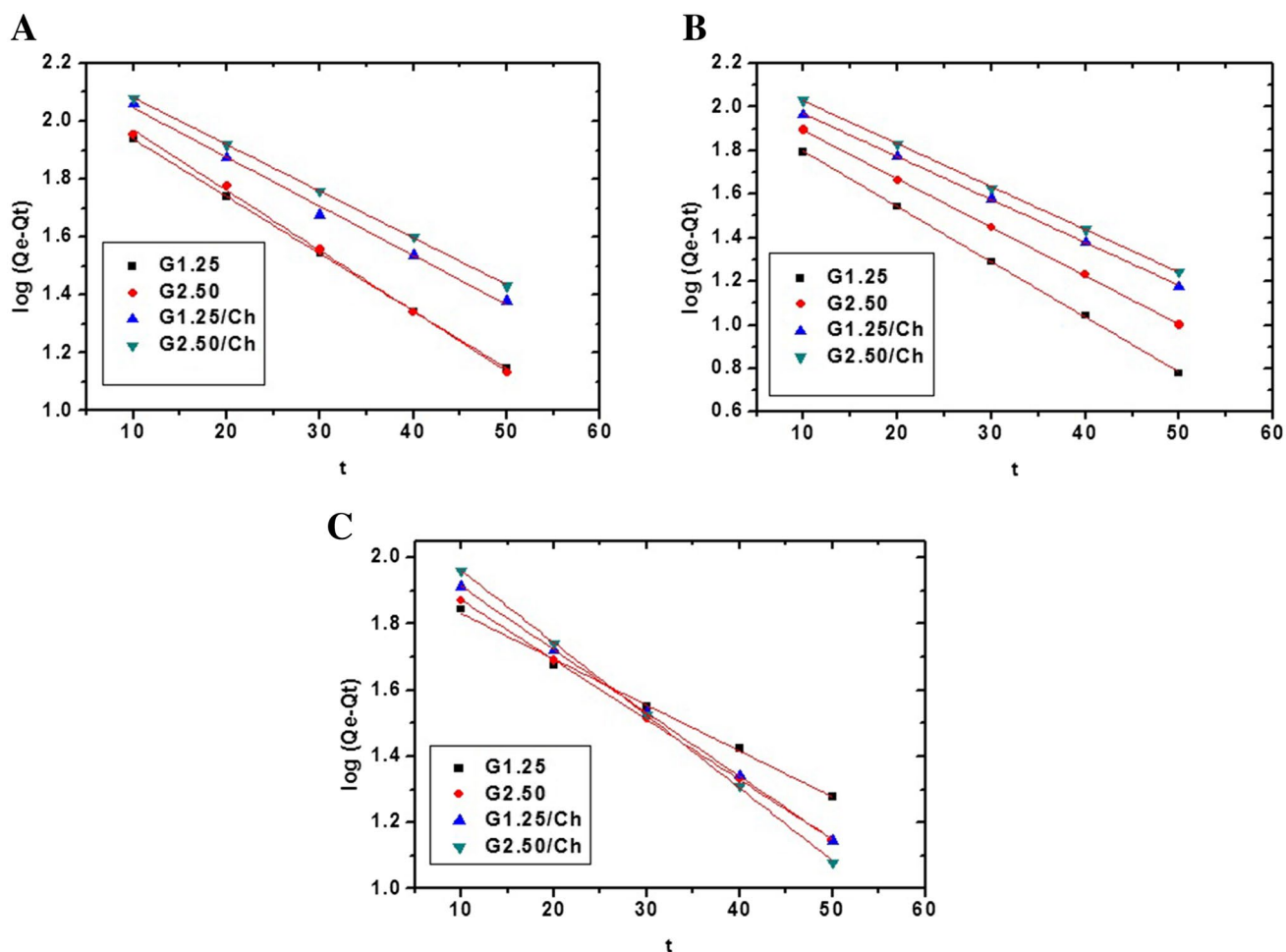
3.2 Removal of Hg(II), Cd(II), or Pb(II) Ions from Aqueous Media

3.2.1 Effect of pH

The amount of adsorbed Hg(II) ions using G1.25, G2.50, G1.25/Ch, and G2.50/Ch was 130, 140, 165, and 175 mg/g at pH 8, respectively as shown in Fig. 5a. The amount of adsorbed Hg(II) ions using the previous adsorbents was decreased by decreasing pH value. The % removal of Hg(II) ions using G1.25, G2.50, G1.25/Ch, and G2.50/Ch was 52, 56, 66, and 70% at pH 8, respectively as shown in Fig. 6a. The % removal of Hg(II) ions using the previous adsorbents was decreased by decreasing pH value.

The amount of adsorbed Cd(II) ions using G1.25, G2.50, G1.25/Ch, and G2.50/Ch was 110, 125, 150, and 160 mg/g at pH 8, respectively as shown in Fig. 5b. The amount of adsorbed Cd(II) ions using the previous adsorbents was decreased by decreasing pH value. The % removal of Cd(II) ions using G1.25, G2.50, G1.25/Ch, and G2.50/Ch was 44, 50, 60, and 64% at pH 8, respectively as shown in Fig. 6b. The % removal of Cd(II) ions using the previous adsorbents was decreased by decreasing pH value.

The amount of adsorbed Pb(II) ions using G1.25, G2.50, G1.25/Ch, and G2.50/Ch was 97.50, 112, 127, and 150 mg/g at pH 8, respectively as shown in Fig. 5c. The amount of adsorbed Pb(II) ions using the previous adsorbents was decreased by decreasing pH value. The % removal of Pb(II)

Fig. 9 Pseudo-first-order for the removal of Hg(II) (**a**), Cd(II) (**b**), and Pb(II) (**c**) ions from aqueous media

ions using G1.25, G2.50, G1.25/Ch, and G2.50/Ch was 39, 44.80, 50.80, and 60% at pH 8, respectively as shown in Fig. 6c. The % removal of Cd(II) ions using the previous adsorbents was decreased by decreasing pH value.

3.2.2 Effect of Time

The amount of adsorbed Hg(II) ions increased with the increase of time till equals 130, 140, 165, and 175 mg/g after 60 min using G1.25, G2.50, G1.25/Ch, and G2.50/Ch, respectively as shown in Fig. 7a. The % removal of Hg(II)

ions increased with the increase of time till equals 52, 56, 66, and 70% after 60 min using G1.25, G2.50, G1.25/Ch, and G2.50/Ch, respectively as shown in Fig. 8a.

The amount of adsorbed Cd(II) ions increased with the increase of time till equals 110, 125, 150, and 160 mg/g after 60 min using G1.25, G2.50, G1.25/Ch, and G2.50/Ch, respectively as shown in Fig. 7b. The % removal of Cd(II) ions increased with the increase of time till equals 44, 50, 60, and 64% after 60 min using G1.25, G2.50, G1.25/Ch, and G2.50/Ch, respectively as shown in Fig. 8b.
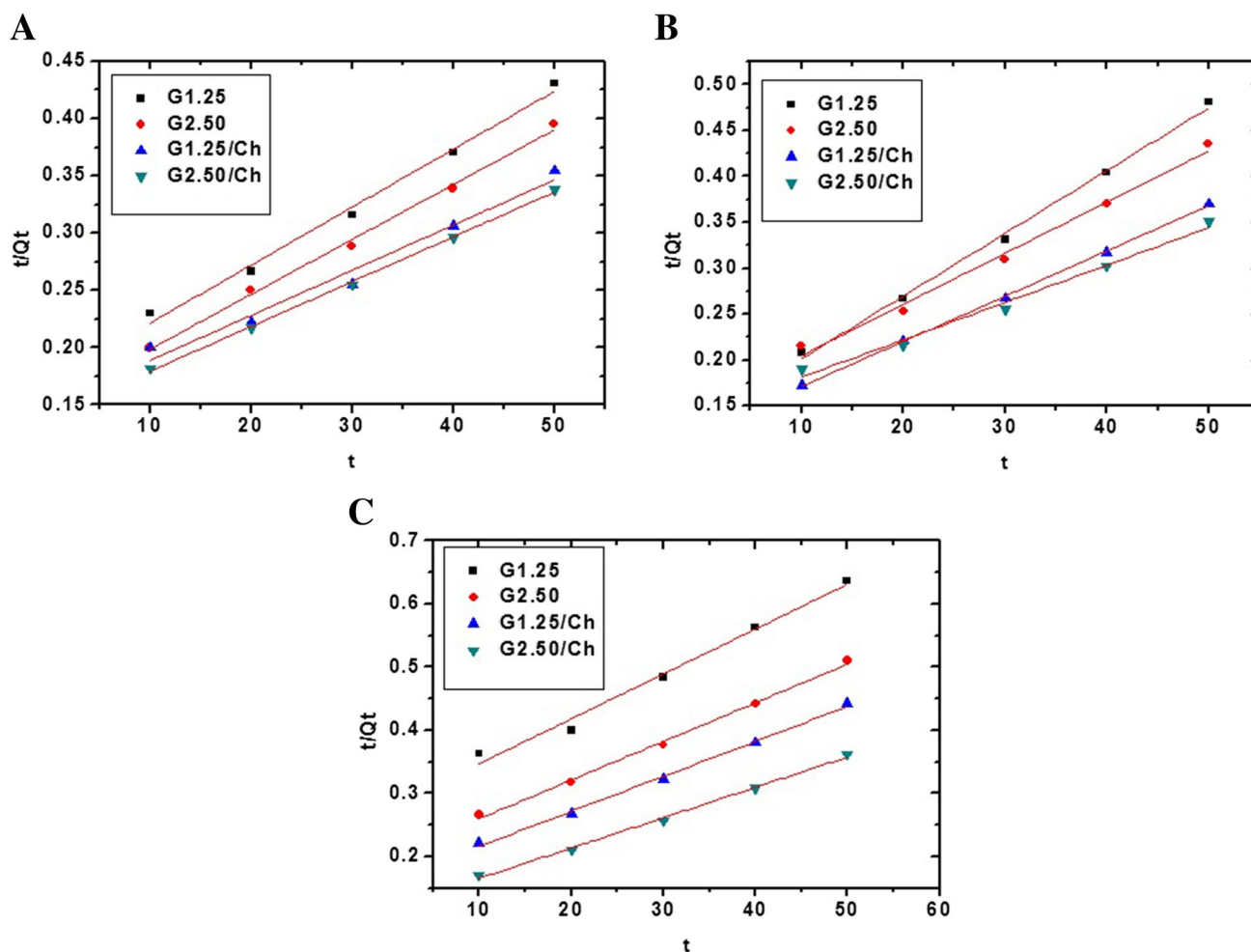
Fig. 10 Pseudo-second-order for the removal of Hg(II) (**a**), Cd(II) (**b**), and Pb(II) (**c**) ions from aqueous media

Table 1 Constants of the applied kinetic models for the removal of Hg(II) ions from aqueous media

Kinetic model	Adsorbent	Constants		
		Q_e (mg/g)	K_F (1/min)	R^2
Pseudo first order	G1.25	136.00	0.046	0.999
	G2.50	150.00	0.048	0.998
	G1.25/Ch	164.27	0.039	0.994
	G2.50/Ch	174.61	0.037	0.999
	Adsorbent	Q_e (mg/g)	K_S (g/mg/min)	R^2
Pseudo second order	G1.25	197.63	1.49E−4	0.989
	G2.50	208.77	1.52E−4	0.995
	G1.25/Ch	253.81	1.04E−4	0.968
	G2.50/Ch	255.75	1.09E−4	0.994

Table 2 Constants of the applied kinetic models for the removal of Cd(II) ions from aqueous media

Kinetic model	Adsorbent	Constants		
		Q_e (mg/g)	K_F (1/min)	R^2
Pseudo first order	G1.25	111.83	0.058	0.999
	G2.50	129.92	0.051	0.999
	G1.25/Ch	146.48	0.045	0.999
	G2.50/Ch	167.61	0.045	0.999
	Adsorbent	Q_e (mg/g)	K_S (g/mg/min)	R^2
Pseudo second order	G1.25	146.63	3.48E−4	0.996
	G2.50	179.53	2.07E−4	0.989
	G1.25/Ch	203.25	1.98E−4	0.988
	G2.50/Ch	246.31	1.176E−4	0.982

Table 3 Constants of the applied kinetic models for the removal of Pb(II) ions from aqueous media

| Kinetic model	Adsorbent	Constants		
		Q_e (mg/g)	K_F (1/min)	R^2
Pseudo first order	G1.25	93.46	0.032	0.996
	G2.50	113.11	0.042	0.999
	G1.25/Ch	127.27	0.044	0.999
	G2.50/Ch	151.87	0.051	0.999
	Adsorbent	Q_e (mg/g)	K_S (g/mg/min)	R^2
Pseudo second order	G1.25	140.85	1.82E−4	0.982
	G2.50	163.39	1.88E−4	0.995
	G1.25/Ch	180.83	1.89E−4	0.996
	G2.50/Ch	207.90	1.97E−4	0.996

The amount of adsorbed Pb(II) ions increased with the increase of time till equals 97.50, 112, 127, and 150 mg/g after 60 min using G1.25, G2.50, G1.25/Ch, and G2.50/Ch, respectively as shown in Fig. 7c. The % removal of Pb(II) ions increased with the increase of time till equals 39, 44.80, 50.80, and 60% after 60 min using G1.25, G2.50, G1.25/Ch, and G2.50/Ch, respectively as shown in Fig. 8c.

To examine the kinetics of adsorption, the pseudo-first-order and pseudo-second-order models were utilized as in Eqs. (3), (4), respectively [22–25].

$$\log \left(Q_e - Q_t\right) = \log Q_e - K_F \, t/2.303 \tag{3}$$

$$t/Q_t = \left(1/K_S \, Q_e^2\right) + \left(1/Q_e\right)t \tag{4}$$

where, Q_t (mg/g) and Q_e (mg/g) are adsorption capacity at time t and equilibrium, respectively. K_S (g/mg/min) and K_F (1/min) are the rate constants of pseudo-second-order and pseudo-first-order models, respectively. The pseudo-first-order linear fitting data due to the removal of Hg(II), Cd(II),
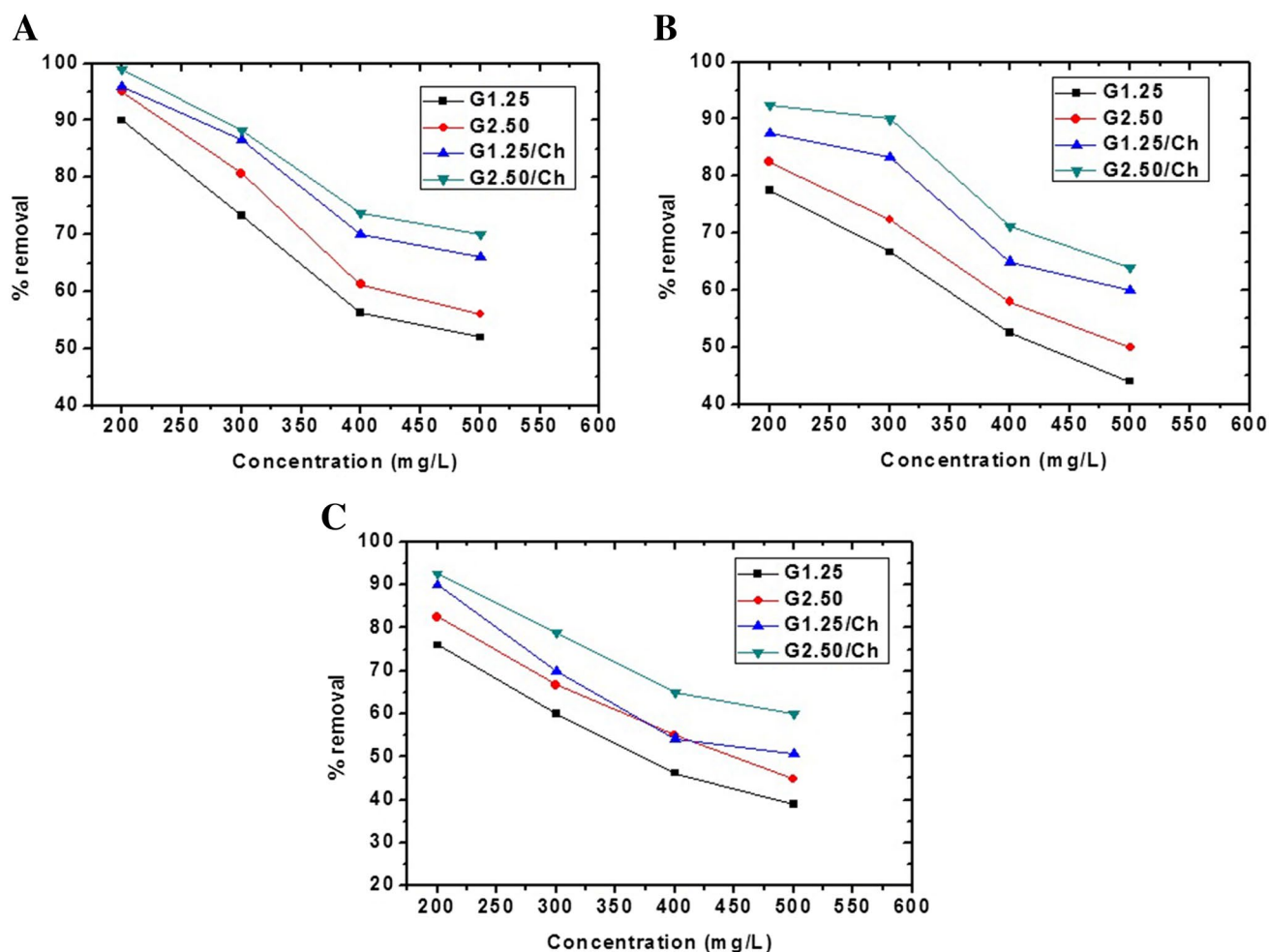
Fig. 11 Relation between concentration and % removal of Hg(II) (**a**), Cd(II) (**b**), and Pb(II) (**c**) ions from aqueous media

and Pb(II) ions have appeared in Fig. 9a–c, respectively. The pseudo-second-order linear fitting data due to the removal of Hg(II), Cd(II), and Pb(II) ions have appeared in Fig. 10a–c, respectively. The determined parameters (i.e. Q_e, K_S, K_F, and correlation coefficient R^2) due to the removal of Hg(II), Cd(II), and Pb(II) ions are displayed in Tables 1, 2, and 3, respectively. The results demonstrate that the determined

Q_e values gotten by the pseudo-second-order model for the adsorption of Hg(II), Cd(II), and Pb(II) ions are not consistent with the experimental Q_e. Also, the determined Q_e values gotten by the pseudo-first-order model are close to the experimental Q_e values.
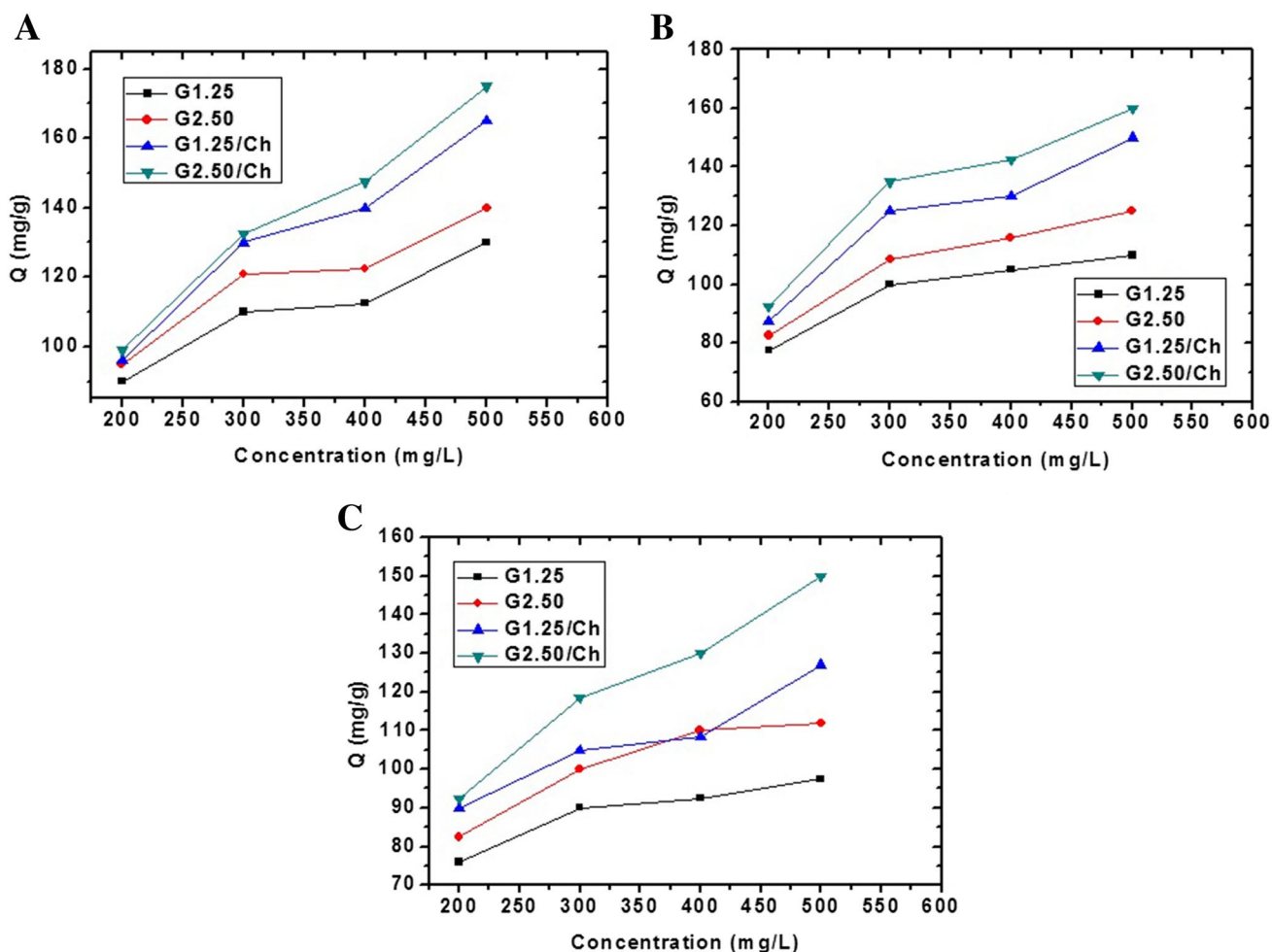
Fig. 12 Relation between adsorption capacity and concentration for the removal of Hg(II) (**a**), Cd(II) (**a**), and Pb(II) (**c**) ions from aqueous media

3.2.3 Effect of Concentration

If the concentration of Hg(II), Cd(II), or Pb(II) ions increases from 200 to 500 mg/L, the % removal decreases as shown in Fig. 11a–c while the adsorption capacity of adsorbents increases as shown in Fig. 12a–c, respectively.

To examine the equilibrium of adsorption, the Langmuir and Freundlich isotherms were utilized as in Eqs. (5), (6), respectively [22–25].

$$C_e / Q_e = \left(1 / K_{Lang} Q_m\right) + \left(C_e / Q_m\right) \tag{5}$$

$$\ln Q_e = \ln K_{Fre} + (1/n) \ln C_e \tag{6}$$

where, Q_m (mg/g) is the maximum adsorption capacity, K_{Fre} (mg/g)(L/mg)$^{1/n}$ is the Freundlich constant, K_{Lang} (L/mg) is the Langmuir constant, and $1/n$ is the heterogeneity factor. Besides, Q_m was determined from Freundlich isotherm using Eq. (7).

$$Q_m = K_{Fre} \left(C_0\right)^{1/n} \tag{7}$$

A

B

C
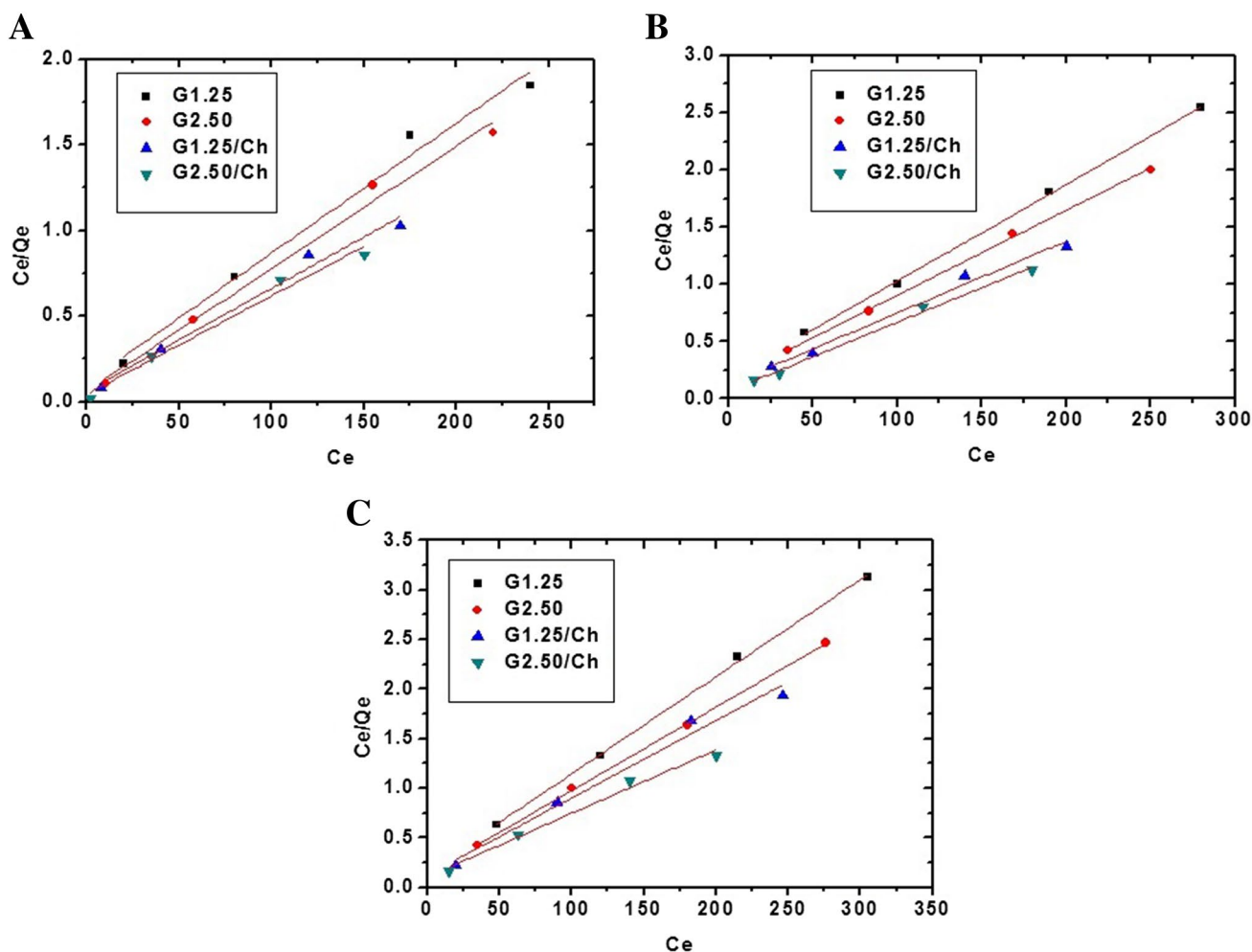
Fig. 13 Langmuir isotherm for the removal of Hg(II) (**a**), Cd(II) (**b**), and Pb(II) (**c**) ions from aqueous media

The Langmuir linear fitting data due to the removal of Hg(II), Cd(II), and Pb(II) ions have appeared in Fig. 13a–c, respectively. The Freundlich linear fitting data due to the removal of Hg(II), Cd(II), and Pb(II) ions have appeared in Fig. 14a–c, respectively. The determined parameters (i.e. Q_m, K_{Lang}, K_{Fre}, and correlation coefficient R^2) due to the removal of Hg(II), Cd(II), and Pb(II) ions are displayed in Tables 4, 5, and 6, respectively. The fitting lines of Langmuir displayed better correlation coefficient than those of Freundlich. Hence, the Langmuir model was more consistent with the removal of Hg(II), Cd(II), or Pb(II) ions from aqueous media. In the case of Hg(II), the maximum adsorption capacity of G1.25, G2.50, G1.25/Ch, and G2.50/Ch were 131.93, 140.85, 166.67, and 173.91 mg/g, respectively. In the case of Cd(II), the maximum adsorption capacity of G1.25, G2.50, G1.25/Ch, and G2.50/Ch were 118.34, 134.95, 159.49, and 166.11 mg/g, respectively. In the case of Pb(II), the maximum adsorption capacity of G1.25, G2.50, G1.25/Ch, and G2.50/Ch were 102.15, 118.91, 128.21, and 156.01 mg/g, respectively.
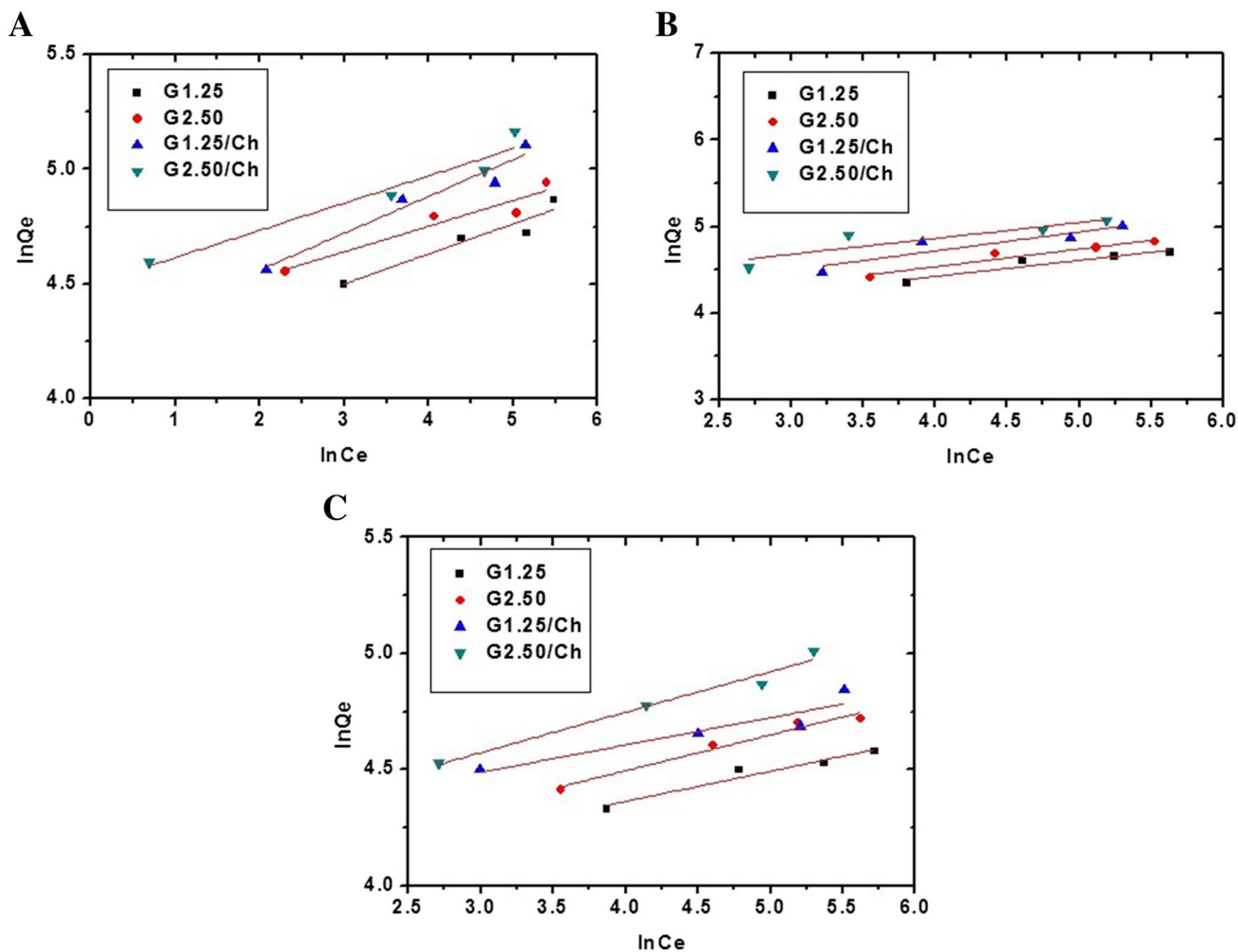
Fig. 14 Freundlich isotherm for the removal of Hg(II) (**a**), Cd(II) (**b**), and Pb(II) (**c**) ions from aqueous media

Table 4 Constants of the applied isotherms for the removal of Hg(II) ions from aqueous media

Adsorption model	Adsorbent	Constants		
		Q_m (mg/g)	K_{Lang} (L/mg)	R^2
Langmuir	G1.25	131.93	0.068	0.979
	G2.50	140.85	0.112	0.985
	G1.25/Ch	166.67	0.096	0.977
	G2.50/Ch	173.91	0.133	0.973
	Adsorbent	Q_m (mg/g)	K_{Fre} (mg/g) (L/mg)$^{1/n}$	R^2
Freundlich	G1.25	137.11	60.89	0.872
	G2.50	148.42	74.09	0.880
	G1.25/Ch	188.38	69.34	0.927
	G2.50/Ch	187.70	89.77	0.915

Table 5 Constants of the applied isotherms for the removal of Cd(II) ions from aqueous media

Adsorption model	Adsorbent	Constants		
		Q_m (mg/g)	K_{Lang} (L/mg)	R^2
Langmuir	G1.25	118.34	0.046	0.999
	G2.50	134.95	0.045	0.998
	G1.25/Ch	159.49	0.051	0.983
	G2.50/Ch	166.11	0.089	0.992
	Adsorbent	Q_m (mg/g)	K_{Fre} (mg/g) (L/mg)$^{1/n}$	R^2
Freundlich	G1.25	126.01	39.64	0.859
	G2.50	146.65	41.37	0.912
	G1.25/Ch	182.44	46.48	0.755
	G2.50/Ch	194.41	62.32	0.693

Table 6 Constants of the applied isotherms for the removal of Pb(II) ions from aqueous media

Adsorption model	Adsorbent	Constants		
		Q_m (mg/g)	K_{Lang} (L/mg)	R^2
Langmuir	G1.25	102.15	0.058	0.999
	G2.50	118.91	0.061	0.999
	G1.25/Ch	128.21	0.063	0.973
	G2.50/Ch	156.01	0.061	0.981
	Adsorbent	Q_m (mg/g)	K_{Fre} (mg/g)(L/mg)$^{1/n}$	R^2
Freundlich	G1.25	104.63	46.64	0.928
	G2.50	125.93	48.27	0.958
	G1.25/Ch	129.89	62.55	0.805
	G2.50/Ch	169.54	57.39	0.959

3.2.4 Effect of Temperature

If the temperature of Hg(II), Cd(II), or Pb(II) solutions increases from 298 to 328 K, the % removal decreases as shown in Fig. 15a–c, respectively. Also, the amount of adsorbed Hg(II), Cd(II), or Pb(II) ions decreases as shown in Fig. 16a–c respectively.

To examine the thermodynamic parameters of adsorption such as a change in free energy ($\Delta G°$), a change in enthalpy ($\Delta H°$), and a change in the entropy ($\Delta S°$), Eqs. (8), (9), were utilized respectively [24, 25, 40, 44].

$$\ln K_d = (\Delta S°/R) - (\Delta H°/RT) \tag{8}$$

$$\Delta G° = \Delta H° - T\Delta S° \tag{9}$$

where, R (KJ/mol K) is gas constant, K_d (L/g) is the distribution coefficient which is estimated utilizing Eq. (10), and T (K) is the temperature of adsorption.

$$K_d = Q/C_e \tag{10}$$

Plotting $\ln K_d$ against T for the removal of Hg(II), Cd(II), and Pb(II) gives $\Delta S°$ and $\Delta H°$ as shown in Fig. 17a–c, respectively. The determined parameters (i.e. $\Delta H°$, $\Delta S°$, and $\Delta G°$) due to the removal of Hg(II), Cd(II), and Pb(II) ions are displayed in Tables 7, 8, and 9, respectively. The values of
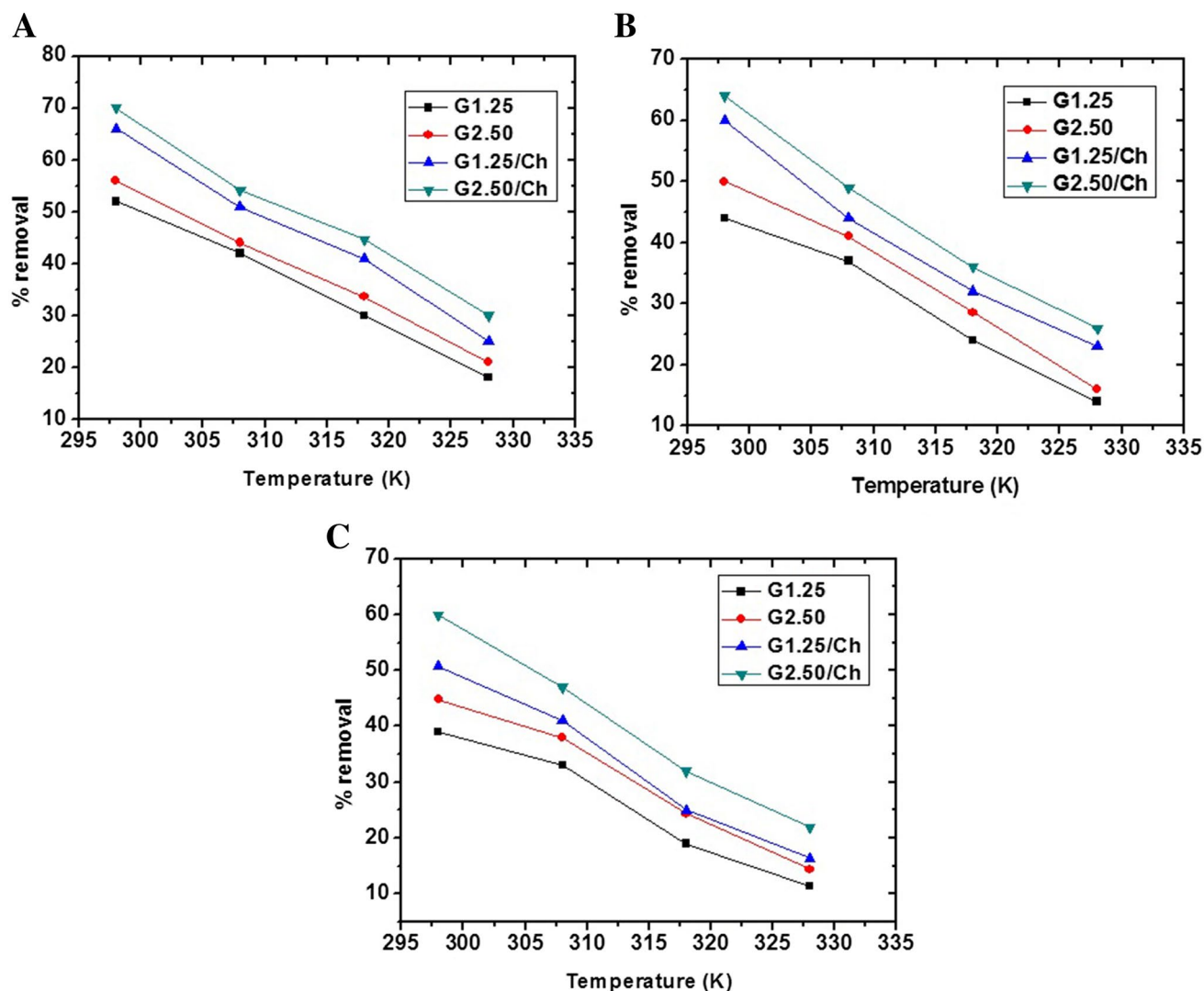
Fig. 15 Relation between temperature and % removal of Hg(II) (**a**), Cd(II) (**b**), and Pb(II) (**c**) ions from aqueous media

$\Delta G°$ for the adsorption of Hg(II), Cd(II), and Pb(II) ions were negative hence the processes were spontaneous. Also, the values of $\Delta H°$ for the adsorption of Hg(II), Cd(II), and Pb(II) ions were negative hence the processes were exothermic. In addition, the values of $\Delta H°$ for the adsorption of Hg(II), Cd(II), and Pb(II) ions were more than 40 kJ/mol hence the processes were chemisorption.

3.2.5 Selectivity Between Metal Ions

The effect of selectivity using the synthesized composites toward Hg(II), Pb(II), and Cd(II) ions was studied as the following:

A mixture of Hg(II), Pb(II), and Cd(II) ions was prepared so that the concentration of each metal inside the mixture equals 200 mg/L. Then, 0.12 g of G1.25/Ch or G2.50/Ch was shaken with 60 mL of the mixture at pH equals 8 for 60 min. After that, the adsorbent was separated then the concentration of Hg(II), Pb(II), or Cd(II) ions in the filtrate was estimated utilizing the atomic absorption spectrometer.

% removal of Hg(II), Pb(II), and Cd(II) ions using G1.25/Ch was 70, 50, and 35, respectively as shown in Fig. 18a. Also, % removal of Hg(II), Pb(II), and Cd(II) ions using G2.50/Ch was 75, 58, and 42, respectively as shown in Fig. 18b.
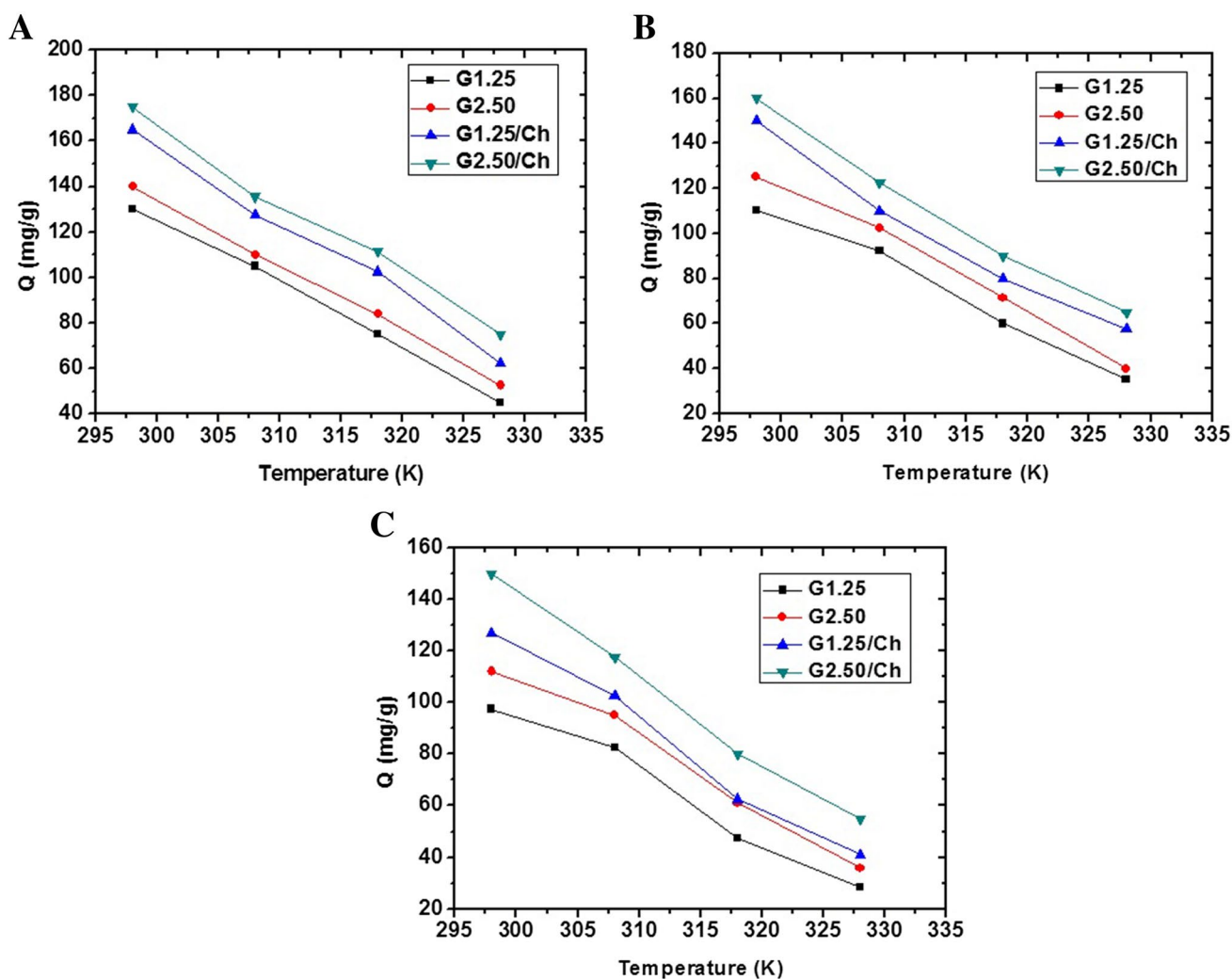
Fig. 16 Relation between adsorption capacity and temperature for the removal of Hg(II) (**a**), Cd(II) (**b**), and Pb(II) (**c**) ions from aqueous media

3.2.6 Comparative Study

A Comparative study was performed between the synthesized composites and other adsorbents in the literature. The adsorption capacity of the synthesized composites exceeds that of many other substances such as natural zeolite, maifanite/MgAl-LDHs, EDTA-LDH/PVA, modified steel-making slag, α-Fe$_2$O$_3$, rice straw, PEI-AC composite, thiol-functional magnetic nanoparticles, ZSM-5 zeolite, magnetite, and hydroxysodalite/Chitosan composite as shown in Table 10 [23, 45–49].

3.2.7 FT-IR Spectra of the Synthesized Composites After Loading with Metal Ions

Figure 19a–c represents the FT-IR spectra of G1.25/Ch composite after loading with Hg(II), Cd(II), and Pb(II) ions, respectively. Also, Fig. 20a–c represents the FT-IR spectra of G2.50/Ch composite after loading with Hg(II), Cd(II), and Pb(II) ions, respectively. Based on the comparison between the FT-IR of G1.25/Ch (Fig. 4b) or G2.50/Ch (Fig. 4d) composite before adsorption and that after adsorption with metal ions as in Fig. 19a–c in the case of G1.25/Ch or the Fig. 20a–c in the case of G2.50/Ch, the
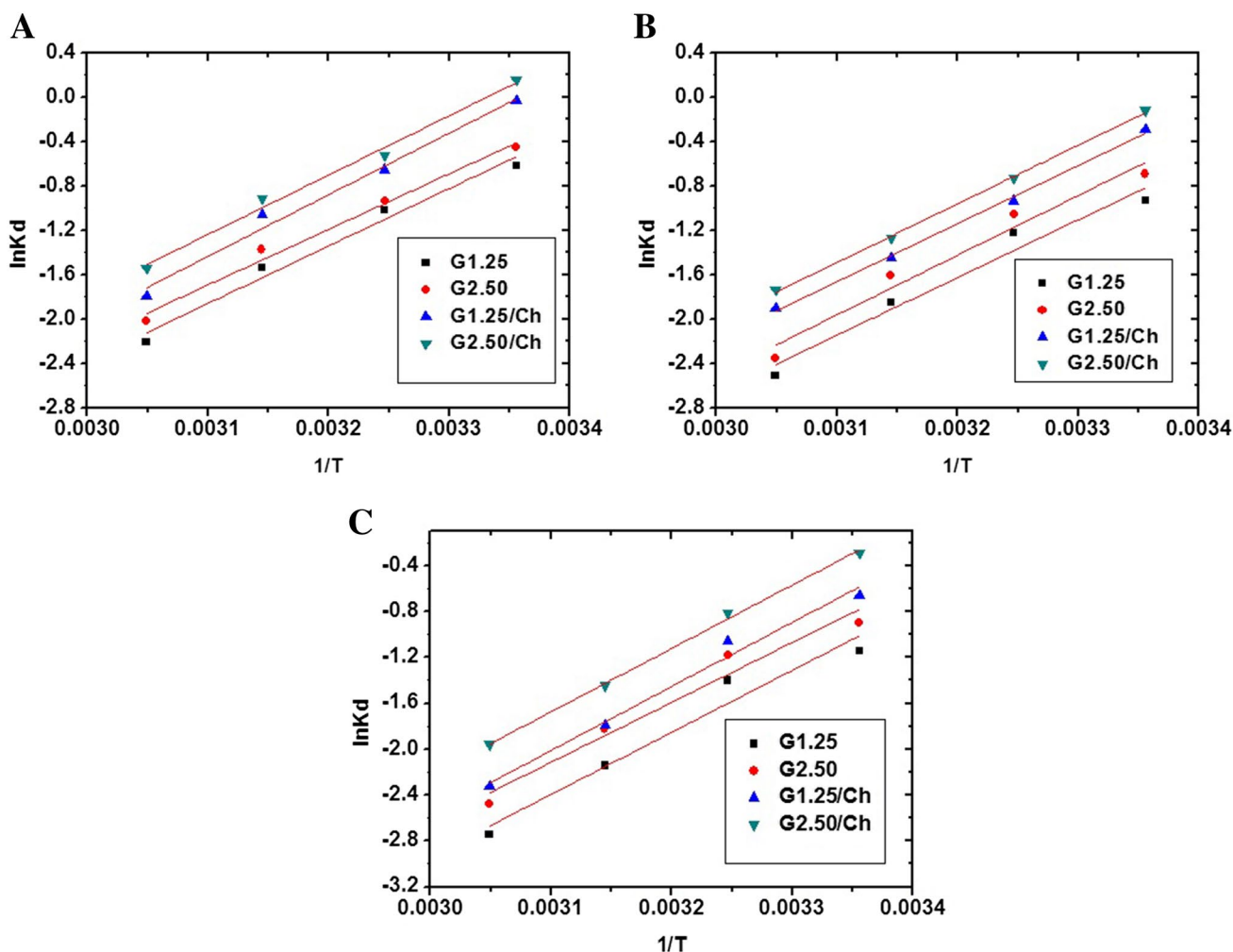
Fig. 17 Relation between ln K_d and 1/T for the removal of Hg(II) (**a**), Cd(II) (**b**), and Pb(II) (**c**) ions from aqueous media

**Table 7** Thermodynamic parameters for the removal of Hg(II) ions from aqueous media

Thermodynamic parameters	$\Delta G°$ (KJ/mol)				$\Delta S°$ (KJ/mol K)	$\Delta H°$ (KJ/mol)
	298 (K)	308 (K)	318 (K)	328 (K)		
G1.25	− 87.65	− 89.14	− 90.63	− 92.12	0.149	− 43.25
G2.50	− 84.79	− 86.23	− 87.67	− 89.11	0.144	− 41.88
G1.25/Ch	− 92.89	− 94.46	− 96.02	− 97.58	0.156	− 46.41
G2.50/Ch	− 89.09	− 90.58	− 92.07	− 93.56	0.149	− 44.69

Table 8 Thermodynamic parameters for the removal of Cd(II) ions from aqueous media

Thermodynamic parameters	$\Delta G°$ (KJ/mol)				$\Delta S°$ (KJ/mol K)	$\Delta H°$ (KJ/mol)
	298 (K)	308 (K)	318 (K)	328 (K)		
G1.25	− 89.03	− 90.56	− 92.09	− 93.62	0.153	− 43.44
G2.50	− 91.42	− 92.98	− 94.54	− 96.10	0.156	− 44.93
G1.25/Ch	− 88.22	− 89.71	− 91.20	− 92.69	0.149	− 43.82
G2.50/Ch	− 88.57	− 90.06	− 91.55	− 93.04	0.149	− 44.17

Table 9 Thermodynamic parameters for the removal of Pb(II) ions from aqueous media

Thermodynamic parameters	ΔG° (KJ/mol)				ΔS° (KJ/mol K)	ΔH° (KJ/mol)
	298 (K)	308 (K)	318 (K)	328 (K)		
G1.25	−92.53	−94.12	−95.71	−97.30	0.159	−45.15
G2.50	−89.18	−90.71	−92.24	−93.77	0.153	−43.59
G1.25/Ch	−94.59	−96.19	−97.81	−99.42	0.161	−46.61
G2.50/Ch	−92.91	−94.48	−96.05	−97.62	0.157	−46.12
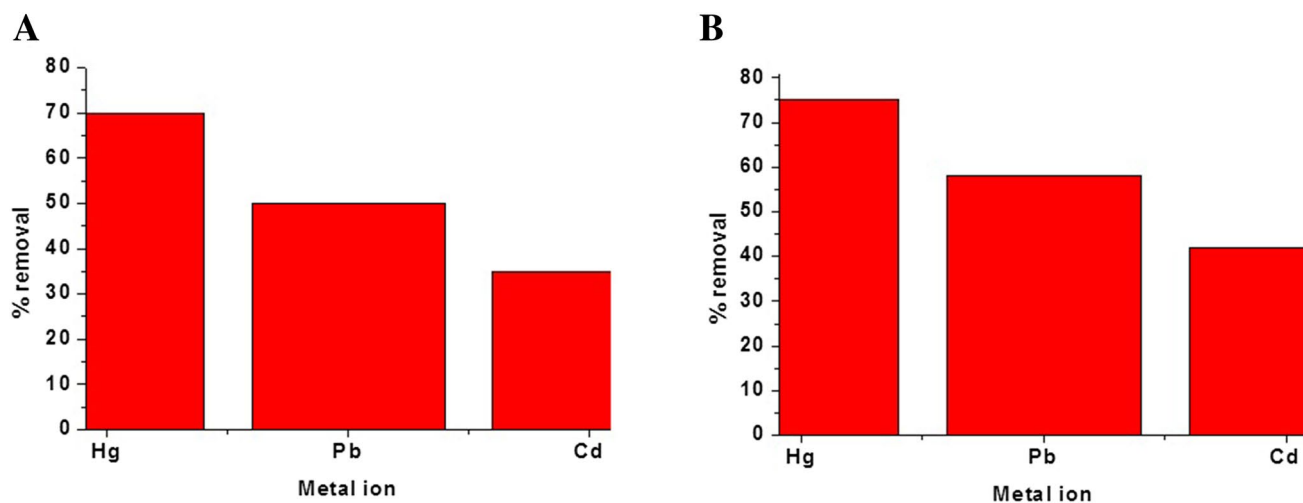
Fig. 18 Selectivity of the G1.25/Ch (**a**) and G2.50/Ch (**b**) composites

Table 10 Comparison between the adsorption capacity of synthesized composites and that for other adsorbents

Metal ion	Adsorbent	Adsorption capacity (mg/g)	References
Cd(II)	Natural zeolite	0.54	[45]
Cd(II)	Maifanite/MgAl-LDHs	3.77	[45]
Cd(II)	EDTA-LDH/PVA	8.18	[45]
Cd(II)	Modified steel-making slag	10.16	[45]
Cd(II)	G1.25/Ch	159.49	This study
Cd(II)	G2.50/Ch	166.11	This study
Hg(II)	α-Fe$_2$O$_3$	11.20	[46]
Hg(II)	Rice straw	22.00	[47]
Hg(II)	PEI-AC composite	16.39	[48]
Hg(II)	Thiol-functional magnetic nanoparticles	9.50	[49]
Hg(II)	G1.25/Ch	166.67	This study
Hg(II)	G2.50/Ch	173.91	This study
Pb(II)	Magnetite	2.78	[23]
Pb(II)	ZSM-5 zeolite	20.10	[23]
Pb(II)	Hydroxysodalite/Chitosan composite	17.85	[23]
Pb(II)	G1.25/Ch	128.21	This study
Pb(II)	G2.50/Ch	156.01	This study

Fig. 19 FT-IR spectra of G1.25/Ch composite after loading with Hg(II) (A), Cd(II) (B), and Pb(II) (C) ions
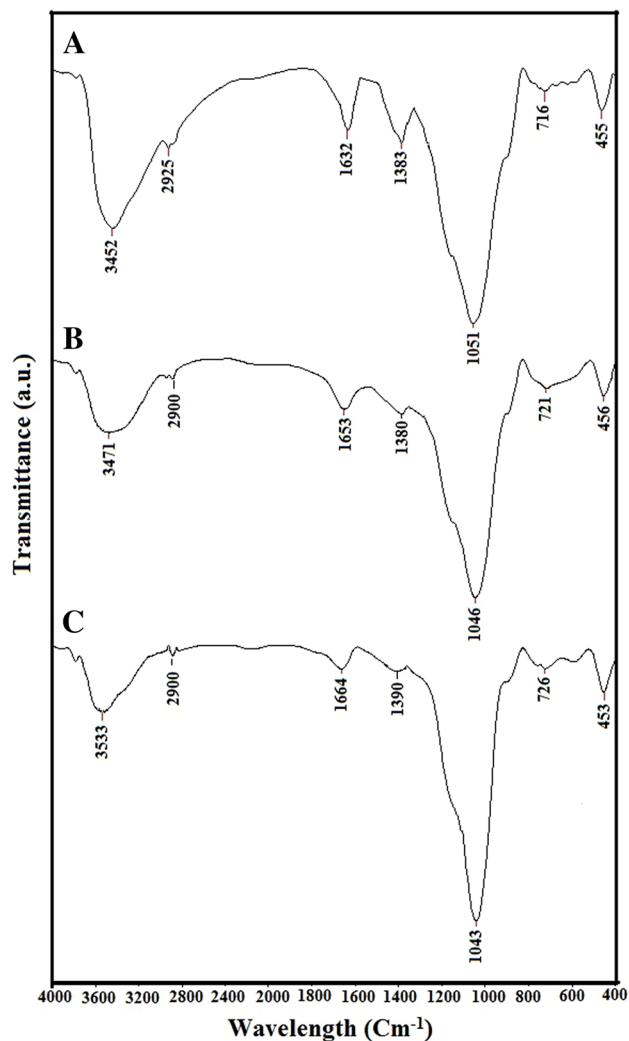
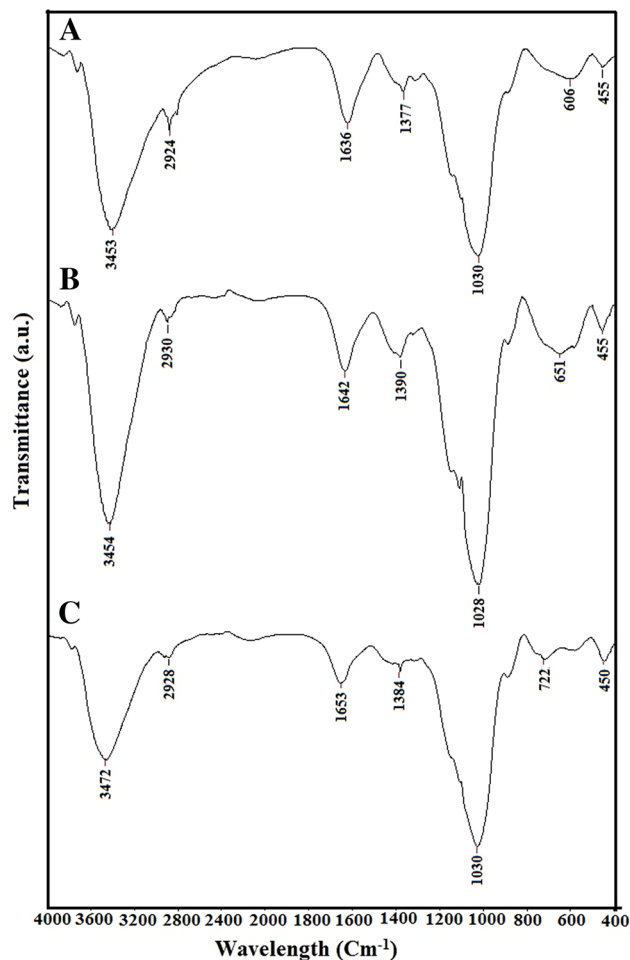Fig. 20 FT-IR spectra of G2.50/Ch composite after loading with Hg(II) (A), Cd(II) (B), and Pb(II) (C) ions

peaks due to NH_2, NH_3^+, C–O of CH_2OH, and T–O–T were shifted to left or right. Hence, they act as binding sites for metal ions [50].

4 Conclusions

Two amorphous aluminum silicates (i.e. geopolymers) were synthesized and modified with chitosan as novel composites. The synthesized geopolymers and their chitosan composites were characterized using different tools such as XRD, FT-IR, SEM, and EDX. Moreover, they were utilized as efficient adsorbents for the removal of Hg(II), Cd(II), and Pb(II) ions from aqueous media.

References

1. E. Nazarzadeh, A. Motahari, M. Sillanpää, Nanoadsorbents based on conducting polymer nanocomposites with main focus on polyaniline and its derivatives for removal of heavy metal ions/dyes: a review. Environ. Res. **162**, 173–195 (2018)
2. Y. Huang, J. Li, X. Wang, Applications of conjugated polymer based composites in wastewater purification. RSC. Adv. **4**, 62160–62178 (2014)
3. S. Jeevanantham, A. Saravanan, R.V. Hemavathy, P.S. Kumar, Removal of toxic pollutants from water environment by phytoremediation: a survey on application and future prospects. Environ. Technol. Innov. **13**, 264–276 (2019)
4. G. Ntombenhle, P. Thabang, M. Meyyappan, K. Moothi, Simultaneous removal of pollutants from water using nanoparticles: a shift from single pollutant control to multiple pollutant control. Sci. Total Environ. **656**, 808–833 (2019)
5. M. Fan, J. Hu, R. Cao, W. Ruan, X. Wei, A review on experimental design for pollutants removal in water treatment with the aid of artificial intelligence. Chemosphere **200**, 330–343 (2018)

6. A.K. Singh, R. Chandra, Pollutants released from the pulp paper industry: aquatic toxicity and their health hazards. Aquat. Toxicol. **211**, 202–216 (2019)

7. C. Aguilar, F. Borrull, E. Fonollosa, A. Nieto, A. Penalver, Presence of radionuclides in sludge from conventional drinking water treatment plants. A review. J. Environ. Radioact. **141**, 24–31 (2015)

8. F. Fu, Q. Wang, Removal of heavy metal ions from wastewaters: a review. J. Environ. Manage. **92**, 407–418 (2011)

9. N.K. Srivastava, C.B. Majumder, Novel biofiltration methods for the treatment of heavy metals from industrial wastewater. J. Hazard. Mater. **151**, 1–8 (2008)

10. D. Sud, G. Mahajan, M.P. Kaur, Agricultural waste material as potential adsorbent for sequestering heavy metal ions from aqueous solutions–A review. Bioresour. Technol. **99**, 6017–6027 (2008)

11. Y. Niu, W. Hu, M. Guo, Y. Wang, J. Jia, Z. Hu, Preparation of cotton-based fibrous adsorbents for the removal of heavy metal ions. Carbohydr. Polym. **225**, 115218 (2019)

12. L. Musab, E.E. Al-Abodi, Preparation and characterization composites contain of magnetic iron oxide nanoparticles with different weight ratios of dextrin, and using it to removal of heavy metals from aqueous solutions. Energy Procedia. **157**, 752–762 (2019)

13. W. Liang, M. Li, S. Jiang, A. Ali, Z. Zhang, R. Li, Polyamine-co-2, 6-diaminopyridine covalently bonded on chitosan for the adsorptive removal of Hg(II) ions from aqueous solution. Int. J. Biol. Macromol. **130**, 853–862 (2019)

14. M. Naushad, T. Ahamad, Z.A. Alothman, A.H. Al-muhtaseb, Green and eco-friendly nanocomposite for the removal of toxic Hg(II) metal ion from aqueous environment: adsorption kinetics & isotherm modelling. J. Mol. Liq. **279**, 1–8 (2019)

15. T. Ahamad, M. Naushad, G.E. Eldesoky, A.A. Alqadami, A. Khan, Synthesis and characterization of egg-albumen-formaldehyde based magnetic polymeric resin (MPR): highly efficient adsorbent for Cd(II) ion removal from aqueous medium. J. Mol. Liq. **286**, 110951 (2019)

16. S. Bao, W. Yang, Y. Wang, Y. Yu, Y. Sun, One-pot synthesis of magnetic graphene oxide composites as an efficient and recoverable adsorbent for Cd(II) and Pb(II) removal from aqueous solution. J. Hazard. Mater. **381**, 120914 (2019)

17. D. Wu, Y. Wang, Y. Li, Q. Wei, L. Hu, T. Yan, R. Feng, L. Yan, B. Du, Phosphorylated chitosan/CoFe$_2$O$_4$ composite for the efficient removal of Pb(II) and Cd(II) from aqueous solution: adsorption performance and mechanism studies. J. Mol. Liq. **277**, 181–188 (2019)

18. Q. Chen, Y. Yao, X. Li, J. Lu, J. Zhou, Z. Huang, Comparison of heavy metal removals from aqueous solutions by chemical precipitation and characteristics of precipitates. J. Water Process Eng. **26**, 289–300 (2018)

19. T. Tran, K. Chiu, C. Lin, H. Leu, Electrochemical treatment of wastewater: selectivity of the heavy metals removal process. Int. J. Hydrogen Energy **42**, 27741–27748 (2017)

20. J.E. Efome, D. Rana, T. Matsuura, C.Q. Lan, Effects of operating parameters and coexisting ions on the efficiency of heavy metal ions removal by nano-fibrous metal-organic framework membrane filtration process. Sci. Total Environ. **674**, 355–362 (2019)

21. M. Qiu, C. He, Efficient removal of heavy metal ions by forward osmosis membrane with a polydopamine modified zeolitic imidazolate framework incorporated selective layer. J. Hazard. Mater. **367**, 339–347 (2019)

22. E.A. Abdelrahman, R.M. Hegazey, Exploitation of Egyptian insecticide cans in the fabrication of Si/Fe nanostructures and their chitosan polymer composites for the removal of Ni(II), Cu(II), and Zn(II) ions from aqueous solutions. Compos. Part B **166**, 382–400 (2019)

23. E.A. Abdelrahman, R.M. Hegazey, Utilization of waste aluminum cans in the fabrication of hydroxysodalite nanoparticles and their chitosan biopolymer composites for the removal of Ni(II) and Pb(II) ions from aqueous solutions: kinetic, equilibrium, and reusability studies. Microchem. J. **145**, 18–25 (2019)

24. E.A. Abdelrahman, D.A. Tolan, M.Y. Nassar, A tunable template-assisted hydrothermal synthesis of hydroxysodalite zeolite nanoparticles using various aliphatic organic acids for the removal of zinc(II) ions from aqueous media. J. Inorg. Organomet. Polym Mater. **29**, 229–247 (2019)

25. E.A. Abdelrahman, R.M.H. Ahmed, Facile synthesis of mordenite nanoparticles for efficient removal of Pb(II) ions from aqueous media. J. Inorg. Organomet. Polym. Mater. (2019). https://doi.org/10.1007/s10904-019-01238-5

26. D. Huang, J. Wu, L. Wang, X. Liu, J. Meng, X. Tang, Novel insight into adsorption and co-adsorption of heavy metal ions and an organic pollutant by magnetic graphene nanomaterials in water. Chem. Eng. J. **358**, 1399–1409 (2019)

27. M.E. Mahmoud, A.A. Yakout, H. Abdel-Aal, M.M. Osman, Enhanced biosorptive removal of cadmium from aqueous solutions by silicon dioxide nano-powder, heat inactivated and immobilized Aspergillus ustus. Desalination **279**, 291–297 (2011)

28. J.G. Outram, S.J. Couperthwaite, G.J. Millar, Enhanced removal of high Mn(II) and minor heavy metals from acid mine drainage using tunnelled manganese oxides. J. Environ. Chem. Eng. **6**, 3249–3261 (2018)

29. J. Hao, L. Ji, C. Li, C. Hu, K. Wu, Rapid, efficient and economic removal of organic dyes and heavy metals from wastewater by zinc-induced in situ reduction and precipitation of graphene oxide. J. Taiwan Inst. Chem. Eng. **88**, 137–145 (2018)

30. M.A. Ahmed, S.M. Ali, S.I. El-Dek, A. Galal, Magnetite-hematite nanoparticles prepared by green methods for heavy metal ions removal from water. Mater. Sci. Eng., B **178**, 744–751 (2013)

31. S.A. Abd El Aal, A.M. Abdelhady, N.A. Mansour, N.M. Hassan, F. Elbaz, E.K. Elmaghraby, Physical and chemical characteristics of hematite nanoparticles prepared using microwave-assisted synthesis and its application as adsorbent for Cu, Ni Co, Cd and Pb from aqueous solution. Mater. Chem. Phys. **235**, 121771 (2019)

32. B. Ranjan, S. Pillai, K. Permaul, S. Singh, Simultaneous removal of heavy metals and cyanate in a wastewater sample using immobilized cyanate hydratase on magnetic-multiwall carbon nanotubes. J. Hazard. Mater. **363**, 73–80 (2019)

33. S.A. Kosa, G. Al-Zhrani, M. Abdel Salam, Removal of heavy metals from aqueous solutions by multi-walled carbon nanotubes modified with 8-hydroxyquinoline. Chem. Eng. J. **181–182**, 159–168 (2012)

34. B. Tan, H. Zhao, Y. Zhang, X. Quan, Z. He, W. Zheng, B. Shi, Amphiphilic PA-induced three-dimensional graphene macrostructure with enhanced removal of heavy metal ions. J. Colloid Interface Sci. **512**, 853–861 (2018)

35. A. Vahdat, B. Ghasemi, M. Yousefpour, Synthesis of hydroxyapatite and hydroxyapatite/Fe$_3$O$_4$ nanocomposite for removal of heavy metals. Environ. Nanotechnol. Monit. Manag. **12**, 100233 (2019)

36. X. Zou, Y. Zhao, Z. Zhang, Preparation of hydroxyapatite nanostructures with different morphologies and adsorption behavior on seven heavy metals ions. J. Contam. Hydrol. **226**, 103538 (2019)

37. S.A. Rasaki, Z. Bingxue, R. Guarecuco, T. Thomas, Y. Minghui, Geopolymer for use in heavy metals adsorption, and advanced oxidative processes: a critical review. J. Clean. Prod. **213**, 42–58 (2019)

38. P. Rożek, M. Król, W. Mozgawa, Geopolymer-zeolite composites: a review. J. Clean. Prod. **230**, 557–579 (2019)

39. H. Luo, W.W. Law, Y. Wu, W. Zhu, E.H. Yang, Hydrothermal synthesis of needle-like nanocrystalline zeolites from metakaolin

and their applications for efficient removal of organic pollutants and heavy metals. Microporous Mesoporous Mater. **272**, 8–15 (2018)

40. E.A. Abdelrahman, R.M. Hegazey, R.E. El-azabawy, Efficient removal of methylene blue dye from aqueous media using Fe/Si, Cr/Si, Ni/Si, and Zn/Si amorphous novel adsorbents. J. Mater. Res. Technol. (2019). https://doi.org/10.1016/j.jmrt.2019.08.051

41. N.B. Singh, S.K. Saxena, M. Kumar, S. Rai, Geopolymer cement: synthesis, characterization, properties and applications. Mater. Today Proc. **15**, 364–370 (2019)

42. E.K. Tiburu, A. Salifu, E.O. Aidoo, H.N.A. Fleischer, G. Manu, A. Yaya, H. Zhou, J.K. Efavi, Formation of chitosan nanoparticles using deacetylated chitin isolated from freshwater algae and locally synthesized zeolite A and their influence on cancer cell growth. J. Nano R. **48**, 156–170 (2017)

43. H.M. Aly, M.E. Moustafa, E.A. Abdelrahman, Influence of aluminum source on the synthesis of nanosized ZSM-5 Zeolite. Der Chem. Sin. **4**, 68–72 (2013)

44. E.A. Abdelrahman, Synthesis of zeolite nanostructures from waste aluminum cans for efficient removal of malachite green dye from aqueous media. J. Mol. Liq. **253**, 72–82 (2018)

45. E.A. Abdelrahman, E.T. Abdel-salam, S.M. El Rayes, N.S. Mohamed, Facile synthesis of graft copolymers of maltodextrin and chitosan with 2-acrylamido-2-methyl-1-propanesulfonic acid for efficient removal of Ni(II), Fe(III), and Cd(II) ions from aqueous media. J. Polym. Res. (2019). https://doi.org/10.1007/s10965-019-1920-4

46. Z. Zhang, H. Liu, P. Lu, T. Chen, W. Ma, Nanostructured α-Fe$_2$O$_3$ derived from siderite as an effective Hg(II) adsorbent: performance and mechanism. Appl. Geochem. **96**, 92–99 (2018)

47. D. Augusto, M. Zaia, R. Ventura, A. Alberto, Use of rice straw as biosorbent for removal of Cu(II), Zn(II), Cd(II) and Hg(II) ions in industrial effluents. J. Hazard. Mater. **166**, 383–388 (2009)

48. T.A. Saleh, A. Sari, M. Tuzen, Optimization of parameters with experimental design for the adsorption of mercury using polyethylenimine modified-activated carbon **5**, 1079–1088 (2017)

49. K. Abbas, H. Znad, M.R. Awual, A ligand anchored conjugate adsorbent for effective mercury (II) detection and removal from aqueous media. Chem. Eng. J. **334**, 432–443 (2018)

50. W.S.W. Ngah, L.C. Teong, R.H. Toh, M.A.K.M. Hanafiah, Comparative study on adsorption and desorption of Cu(II) ions by three types of chitosan–zeolite composites. Chem. Eng. J. **223**, 231–238 (2013)